Energy Conversion and Management 88 (2014) 498–515

Contents lists available at ScienceDirect

Energy Conversion and Management

journal homepage: www.elsevier.com/locate/enconman

Economic–environmental hierarchical frequency management of a droop-controlled islanded microgrid

Navid Rezaei, Mohsen Kalantar *

Center of Excellence for Power Systems Automation and Operation, Electrical Engineering Department, Iran University of Science and Technology (IUST), Tehran, Iran

ARTICLE INFO

Article history:
Received 30 May 2014
Accepted 24 August 2014

Keywords:
Microgrid energy management system
Frequency control
Droop method
Reserve scheduling
Hierarchical control

ABSTRACT

This paper presents a novel energy management system (EMS) for a microgrid to enhance the power system security in a cost-effective manner. Small size of the islanded microgrids, high levels of intermittency and energy fluctuations, lower inertia potential of inverter-interfaced distributed energy resources (DERs) makes the frequency a vital factor in the microgrid energy management system that should be managed subject to the economic–environmental policies of the microgrid EMS. The proposed model is based on precise energy and reserve scheduling of the DERs in a droop-controlled islanded microgrid to manage the possible microgrid frequency excursions. The expected value of the microgrid frequency excursions stem from system power deviations is employed as a new objective function in this study, which is aimed to be minimized using a two stage stochastic mixed-integer linear programming method. In order to model the hierarchical control structure of the islanded microgrid, the frequency dependent behavior of the droop-controlled inverter-interfaced DERs is formulated thoroughly. The proposed model is applied to a typical microgrid test system. The primary and secondary frequency control reserves are appropriately scheduled over a 24 h period. A methodology based on the Monte-Carlo simulation strategy is adapted to generate some random scenarios corresponding to renewable generation variations, load consumption deviations and contingencies of line/unit outages. The generated scenarios are reduced and applied to the optimization approach. Moreover, using the proposed hierarchical control structure, the microgrid frequency excursions are managed aptly in predefined acceptable ranges by readjusting the reference power set-points of dispatchable DERs. Numerical results and detailed analyses effectively verify the great importance of the frequency control modeling in the energy and reserve management problem of the microgrids.

1. Introduction

Recently, in order to promote the sustainability and reliability of the power systems subject to economic and environmental consciousness, the concept of smart grid has been presented. In order to support this idea, distributed energy resources (DERs) are widely exploited in the power systems. The operation of the DERs is more salient in the distribution side of the power systems, closer to the end-user consumers. In this scheme, microgrids can play as controllable aggregators to actively manage variety of the DERs in small islanded or grid-connected power distribution systems [1]. Microgrids not only alleviate the deteriorative impacts of individual non-cooperative exploitation of the DERs, but also providing high quality energy services in accordance to the smart grid eventual goals [2,3]. Achievement of these functions necessitates the presence of an energy management system (EMS) to procure security and controllability issues in promising levels [4]. Functionally, EMS in a microgrid is in charge of appropriate synchronization with the main grid, robust damping of the microgrid disturbances, optimal power sharing among DERs and providing efficient power set points. Through appropriate control functions, the EMS insures the microgrid power balance requirement and consequently maintaining the system frequency stability [1–3].

Owing to the small scale power capacity of the microgrids, frequency is critically exposed to severe deviations. This will cause extensive load tripping and increase the risk of the possible system damages. Indeed, system security significantly has greater importance in the microgrids, because the philosophy of the microgrid concept is to procure a sustainable, clean and economical energy for the consumers. Thus, frequency is a key control factor in the microgrid management system [4–6]. As a result, properly control of the microgrid frequency not only guaranties itself security but

* Corresponding author. Address: Narmak, Tehran, Postal code: 1684613114, Iran. Tel.: +98 2173225662; fax: +98 2173225662.

E-mail addresses: nrezaei@iust.ac.ir (N. Rezaei), kalantar@iust.ac.ir (M. Kalantar).

http://dx.doi.org/10.1016/j.enconman.2014.08.054
0196-8904/

Nomenclature

Acronyms

DER	distributed energy resource
DG	distributed generation
DSO	Distributed System Operator
ELNS	Expected Load Not Served
EMS	energy management system
ESF	expected system frequency
LC	Local Controller
LMCS	Lattice Monte Carlo Simulation
MGCC	Micro-Grid Central Controller
MILP	mixed-integer linear programming
MINLP	mixed-integer non-linear programming
RES	renewable energy source
RWM	Rolette Wheel Mechanism
TSC	Total System Cost
TSE	Total System Emission
VOLL	value of lost load

Indices

i	index of dispatchable distributed generation units (DGs) from 1 to Ng
w	index of wind turbines from 1 to Nw
v	index of photovoltaic panels from 1 to Nv
s	index of scenarios from 1 to Ns
h	index of hours from 1 to Ns
m	index of frequency control level could be equal to *pri* (primary) and *sec* (secondary)
q	index of scheduled reserves could be *up* or *down*

Parameters and constants

$m_p(i)$	frequency droop parameter of DG i
f_{ref}	microgrid reference frequency
Δf_m^{max}	maximum allowable microgrid frequency excursion limit during control level m
a_i	fixed operation cost of DG i
b_i	first-order operation cost of DG i
SUC_i	start-up cost of DG i
SDC_i	shut-down cost of DG i
$\rho_i(m,q)$	cost up/down reserve of DG i in control level m
ρ_w	cost of operation of wind turbine w
ρ_v	cost of operation of photovoltaic panel v
$P_g^{max}(i)$	upper level of active power generation of DG i
$P_g^{min}(i)$	lower level of active power generation of DG i
RU_i	ramp-up limit of DG i
RD_i	ramp-down limit of DG i
RSU_i	start-up ramp of DG i
RSD_i	shut-down ramp of DG i
TUP_i	minimum up time of DG i
TDN_i	minimum down time of DG i
$E_i^{CO_2}$	CO_2 emission rate of DG i
$Load(h)$	forecasted load consumption at hour h
$P_w(w,h)$	forecasted active power output of wind turbine w at hour h
$P_v(v,h)$	forecasted active power output of photovoltaic panel v at hour h
δ_i^0	initial online hours of DG i at hour 0
σ_i^0	initial offline hours of DG i at hour 0

Variables

π_s	probability of scenario s
$\Delta f(s,m,h)$	microgrid frequency deviation in scenario s, control level m and at hour h
$u^m(i,h)$	binary variable indicating commitment state of DG i at hour h and control level m
$\Delta P_g(s,i,m,h)$	active power deviation of DG i in scenario s, control level m and hour h
$\Delta P_w(s,w,m,h)$	active power deviation of wind turbine w in scenario s, control level m and hour h
$\Delta P_v(s,v,m,h)$	active power deviation of photovoltaic panel v in scenario s, control level m and hour h
$\Delta Load(s,m,h)$	active power deviation of microgrid load in scenario s, control level m and hour h
$W_{i,h,s}^{DG}$	binary variable indicating availability status of DG i in scenario s and hour h
$P_g(i,h)$	Active power output of DG i at hour h
$D(s,m,h)$	frequency elasticity of microgrid loads in scenario s, control level m and hour h
$P_{ref}(i,h)$	reference power set point of DG i at hour h
$R_g(i,m,q,h)$	scheduled up/down reserve of DG i in control level m and hour h
$Load^s(m,h)$	microgrid load consumption in control level m and hour h
$P_g^s(i,m,h)$	active power output of DG i in scenario s, control level m and hour h
$P_{ref}^s(i,m,h)$	reference power of DG i in scenario s, control level m and hour h
$P_w^s(w,m,h)$	active power output of wind turbine w in scenario s, control level m and hour h
$P_v^s(v,m,h)$	active power output of photovoltaic panel v in scenario s, control level m and hour h
$LSH(s,m,h)$	load to be shed unwillingly in scenario s, control level m and hour h
$u(i,h)$	binary variable indicating commitment state of DG i at hour h
$y(i,h)$	binary variable indicating start-up state of DG i at hour h
$z(i,h)$	binary variable indicating shut-down state of DG i at hour h

also helps saving the whole power system from undesirable blackout events. In a microgrid, the frequency excursions can easily stem from the renewable energy sources (RES) intermittent nature, load demand variations and possible lines/units outages. Besides, due to the characteristics of the produced energy from heterogeneous energy resources, the DERs are often connected to the microgrid via power electronic devices commonly known as static voltage source inverters (VSIs) [7]. Therefore, the microgrids usually suffer from low inertia stack which may increase its vulnerability in contrast to frequency deviations. Additionally, owing to the considerable ratio of the power fluctuations to the load served in the microgrids, it seems that the system frequency changes faster and more unpredictably with respect to the conventional synchronous generator based power systems. The problem is more crucial in the islanded microgrids, since in the grid connected mode, microgrid can rely on the main grid as a major power source to compensate its inherent power variations. Therefore, role of the EMS to control the system frequency in a cost-effective manner and in compliance to the environmental agreements seems to be crucial. In other words, the EMS is responsible to schedule DERs in such a way that after any disturbances, there will be enough reserves to manage the system frequency. Concisely, in the islanded mode, precise reserve management strategy is a significant challenge needs to be investigated more thoroughly.

Generally, energy management system in a microgrid can be implemented in a centralized or decentralized manner. In the centralized structure, Microgrid Central Controller (MGCC) plays the most prominent role in the EMS. The MGCC can be considered as an interface between the Distribution System Operator (DSO) and microgrid internal Local Controllers (LC) [1–3,8]. Despite the decentralized operation in which decisions are determined locally, in the centralized approach, the operational decision makings are performed through the MGCC. The control functions of a microgrid can be implemented through a hierarchical control structure. Similar to the conventional power systems, the hierarchical control of the microgrids consists of primary, secondary and tertiary levels [9–11]. Primary control plays as a distributed automatic control in each DER and procures primary control reserves proportionally to the system frequency deviations. Secondary control reserves are activated after the primary interval by adjusting the microgrid DER set points to restore the system frequency to its rated value. It is worth to be mentioned that tertiary control level is responsible to control the power exchanges with the main grid and provision an optimistic energy dispatch in the microgrid [12–15]. Notably, the tertiary control approximately has similar functions as the secondary level and covers all other control levels [5,6].

To ensure the security, power balance and load sharing in the islanded microgrids, appropriate control functions should be applied to the interfaced VSIs. Especially, in the islanded microgrids, the DERs should share the active power requirements properly such a way the undesired circulating currents between the parallel VSIs are avoided and also the VSIs are preserved of the thermally overstressing risks [16]. Though, in the last decades, several control techniques, such as master/slave, current/power sharing and other hybrid methods were implemented to control the VSIs [17], recently, the researchers have been more interested in the employment of the so-called droop control method. The original concept of the droop controllers was first introduced by Chandorkar et al. in 1993 [18]. Principally, the cornerstone of the droop control is emulation of the behavior of the synchronous generators using an inverse relation between injected active power and the system frequency without the need to a massive communication infrastructure [15]. Indeed, *P–f* droop control facilitates decision makings on the control actions to control the power balance on account of the possibility of locally measuring the microgrid frequency [19]. Indeed, automatic droop based controllers serve to mitigate frequency deviations by releasing proper frequency control reserves which can be scheduled by means of the EMS. Obviously after any system imbalances, the steady-state frequency may deviate from its nominal value, hence, the MGCC can perform as a supervisory control in the EMS to restore the system frequency to its nominal value while satisfying the microgrid optimal operational purposes [4,12]. In gist, provision of good performance in accost of significant renewable energy and system load variations, makes the necessity of a robust energy management system integrated with the real-time control strategy and optimal day-ahead energy and reserve scheduling be indispensible.

Although in the last two decades, several researches have been dedicated to the microgrid energy management issues [20], there is still a need of further investigation to thoroughly inquire into the microgrid optimal energy management strategies, particularly with emphasize on frequency control issues. Optimal day ahead operational planning of a grid connected microgrid using heuristic based optimization algorithms were studied in [21–30]. The proposed EMS systems consider the microgrid energy dispatch subject to the economic and/or environmental objectives in either deterministic [21–24] or scenario-based stochastic [25–27] or based on Hong's point probabilistic [28–30] frameworks. Besides, to cope with the microgrid uncertainty resources, authors in [31,32] have also investigated a cost-effective methodology to determine the capacity of an energy storage using sensitivity analysis [31] and model predictive control [32] approaches. However, the effects of the microgrid static frequency on the all mentioned energy management systems were ignored.

Furthermore, the EMS in the islanded [33,34] and grid-connected [35,36] microgrids using a mathematical based mixed-integer nonlinear programming (MINLP) optimization method has been investigated in order to maximize the DERs utilization in the light of properly dispatching energy and reserve resources and achieving the lower price of energy to the end-user active consumers. However, the MINLP models have deficiencies in ensuring the feasibility and global optimality of the solution. Proposing a mixed-integer linear programming (MILP) based EMS has been examined in [37] using a simplified rolling horizon strategy. Despite the efficiency of the proposed energy management systems, the focus of these papers are mainly on upper level of the energy management system, i.e. functions related to the MGCC, and the performance of lower energy management level in the terms of the LCs' performance has been neglected. Obverse, investigation of the optimal real time power sharing management between the DER units in the islanded microgrids considering to short time based economic criteria has been presented in [38–40]. Refs. [38–40] focused on the dynamic stability satisfaction of the droop-regulated microgrids. The real-time fuel cost was minimized subject to dynamic stability restrictions. These studies have not considered the great role of the non-dispatchable DG units (e.g. wind turbines or photovoltaic panels) in the energy management strategies. Furthermore, long-term operational planning in terms of the day-ahead energy and reserve scheduling is ignored in those droop regulated systems. Authors in [12,41] through proposing efficient control strategies for islanded microgrids, evaluate the role of a centralized energy management system in minimizing the microgrid frequency excursions. However, their objective functions were rather on the basis of the dynamic response of the DERs to the transient disturbances, while the present paper, aims to optimize the microgrid day ahead steady-state frequency profile.

Ref. [42] presented a two layer energy management strategy to energy and reserve scheduling of the DERs in a 24 h period. The scheduling errors were corrected in the 15 min dispatching intervals. Again, the performance of the system frequency controllers has not been modeled. In eligible work presented in [43] a hierarchical centralized energy management system has been proposed. The model well described the performance of the MGCC and LCs through an optimal energy scheduling program. However, system uncertainties and their impacts on the microgrid frequency have not been investigated. Beside, the proposed optimization was based on the evolutionary algorithms which usually suffer from the constraint handling, particularly in the large scale high constrained problems.

The paper approach focuses on proposing an efficient energy management system by precise modeling of the frequency based droop controller behavior of the inverter interfaced distributed generation units. Also, impacts of the renewable energy source intermittencies and load fluctuations on the system frequency excursions are modeled using a two-stage stochastic programming which is aimed to be solved by means of an efficient MILP method that guaranties achieving the near-optimal solution. In the first stage, random scenarios related to the system RES and load forecasting errors are generated and properly reduced using Roulette Wheel Mechanism (RWM) and Lattice Monte Carlo Simulation (LMCS) strategies. In the second stage, the proposed MILP frequency control optimization is performed over the reduced scenarios considering to the system operational restrictions. Concisely, the EMS schedules an islanded microgrid energy and reserve resources in a day-ahead optimization in which system frequency deviations are minimized subject to the economic and environmental operational constraints pre-specified by mean of the EMS. The EMS through monitoring the microgrid energy flows tries to schedule the LCs and MGCC in such a way that there will be enough reserve resources to cover the possible system frequency excursions caused stochastically by the generation and load deviations or DG outages. Hence, LCs automatically release their primary reserve capacities, then, the MGCC by applying a security constraint unit commitment program adjusts the set points of the dispatchable DG units to minimize the microgrid steady-state frequency excursions caused by the LCs' primary control action. Meanwhile the MGCC provides the microgrid cost and emission requirements. In summary, the main contributions of the paper can be highlighted as:

- The steady state frequency of the microgrid is analyzed in-depth by modeling the behavior of the droop controlled VSI-based DERs. The primary and secondary control levels of the hierarchical frequency management structure will be formulated comprehensively.
- A novel objective function based on the day-ahead frequency profile of the microgrid is proposed for the first time. The frequency-based objective function is linearized using an efficient technique and aimed to be minimized using a mixed-integer linear programming approach.
- Both primary and secondary frequency control reserves are scheduled properly through a well-organized two-stage scenario-based stochastic framework.

The remainder of the paper is organized as follows. Section 2 presents an overview of the microgrid hierarchical control and energy management structure. The load–frequency control principles of the inverter-interfaced DG units are investigated precisely. The formulation and model description of the proposed two-stage stochastic MILP frequency control optimization is studied thoroughly in Section 3. In Section 4, the suggested energy management system is applied to an islanded microgrid and the numerical results are analyzed and the efficiency of the proposed hierarchical frequency control is evaluated. Finally, in Section 5, concluding remarks are discussed.

2. Overview of microgrid hierarchical control structure

Similar to the conventional power systems and owing to the distinctive control tasks and time constants in microgrid operation, a hierarchical control structure can be employed into the frequency management of the microgrids. Indeed, microgrid operational goals can be achieved through a hierarchical three level based energy management structure which is performed in either centralized or decentralized way [44]. In the decentralized structure, microgrid optimal operation is provided using a high level of autonomy and usually performed based on multi-agent systems. In the centralized control, the real time and forecasting data of the microgrid are utilized by means of a central supervisory controller to determine the dispatch of the DERs. In islanded microgrids, motivated by high level of sophisticated control required for various DERs, the centralized control is preferred [45].

The primary control level encompasses the LC functions which are responsible of properly control the DER units and some controllable loads as well as pursuing the microgrid power balance through a proper power sharing procedure. The MGCC lies on the second control level employed in order to ensure the microgrid reliable operation subject to the economic, environmental and security policies of the EMS. The secondary control can be also treated as energy management system (EMS). In the islanded microgrids, the secondary control is the highest control level [45]. In the tertiary control level, DSO is in charge of control power interactions between the microgrid and the up-stream distribution power system, coordination between several microgrids and providing suitable market participation of the multi-microgrids [4–8,44,45]. Concepts of the load–frequency control in the synchronous generators have been presented thoroughly in [46–48].

According to the droop control basis, the microgrid frequency and voltage deviations are regulated regarding to the active and reactive power deviations, respectively. Eqs. (1) and (2) present P–f and Q–V droop based control methods applied to the inverter interfaced DER units, respectively [12–14]:

$$f = f_{ref} - m_p(P_g - P_{ref}) \quad (1)$$

$$V = V_{ref} - m_q(Q_g - Q_{ref}) \quad (2)$$

where f, f_{ref}, V and V_{ref} are the microgrid frequency, frequency reference value, voltage amplitude of the VSI and voltage reference value of the VSI, respectively, P_g, P_{ref}, Q_g and Q_{ref} are active power output, reference active power set point, reactive power generation and reference reactive power set point of DG units, respectively. m_p and m_q are droop gain of the frequency and voltage droop controllers, respectively. The emphasis of the present paper is only on the frequency droop control of the inverter interfaced DG units and investigation of the Q–V droop control is not in the scope of the paper. In other words, it is assumed that these two droop based controllers are decoupled [17]. The droop control block-diagram of an inverter interfaced DG unit is illustrated in Fig. 2. In the steady-state analysis, it is assumed that the system dynamics including the transient and oscillating modes are all damped out and power system is reached to a stable equilibrium point.

Obviously, as illustrated in Fig. 1, any deviations in the microgrid active and reactive power reference values cause voltage and current of the VSI to be changed as ΔV_g and ΔI_g. Next the active/reactive power calculation block (PQC) measures the power deviations using ΔV_g and ΔI_g measurements and through using a low-pass filter. In this stage LC which sensed the deviations is activated to compensate the active and reactive power deviations by adjusting frequency and voltage magnitude of the VSI, respectively, in a real-time and automatic way. Newly generated frequency and voltage magnitude for the VSI, i.e. f^* and $|V|^*$, are properly regulated in the VSI internal current (F_I) and voltage (F_V) controllers such that the final reference voltage phasor (V^*) for the VSI be produced in a stable way. The VSI using a suitable Pulse Width Modulation (PWM)-based switching control technique generates the desired voltage level by absorbing the ΔP_{vsi} from DC link energy storage. The generated VSI power ($\eta \cdot \Delta P_{vsi}$) is injected to the interconnecting microgrid ac bus as presented by ΔP_g. It should be noted that in this paper, it is assumed that the drop in the DC link voltage (V_{dc}) due to the absorbed VSI active power is negligible and the DG primary source will feed the VSI demands without any considerable DC link voltage drops, i.e. it is assumed that $\Delta P_{ps} \approx \Delta P_{vsi}$. Notably, the proposed modeling is derived under the assumption that all the transients and oscillating modes have been damped out and the system reached to a new steady-state condition. As mentioned above, it is assumed that there is an analogous mechanism for the reactive power regulation which is performed in a decoupled way and the voltage deviations arise from the reactive power output variations of the microgrid components are ignored in this study.

As it is described, frequency droop control method makes DG units behave as the conventional synchronous generators [8], i.e. the VSI frequency droop controller performs exactly as the governors of the synchronous generators and regulates system frequency deviations in proportional to the active power changes. In other words, whenever there are any power deviations in the microgrid, caused either by renewable energy resources and load

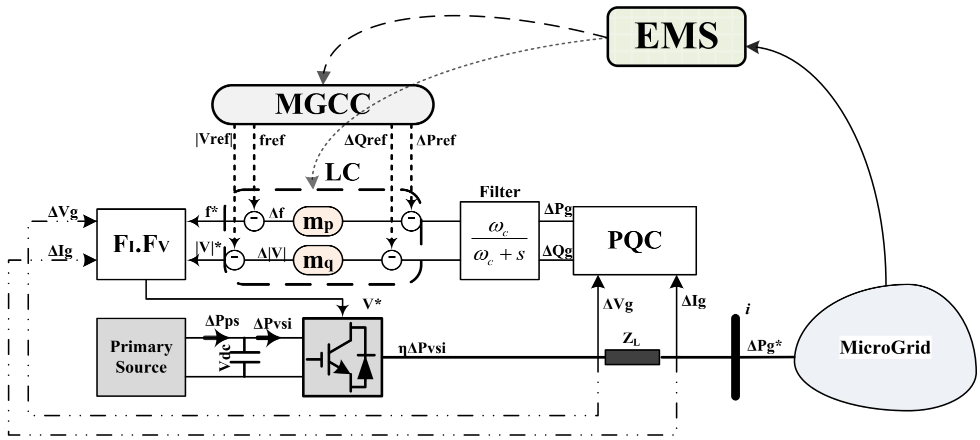

Fig. 1. The diagram of a droop controlled inverter-interfaced distributed generation hierarchical frequency control structure.

fluctuations or units/lines contingency events, accordingly the *P–f* droop control loop changes the frequency of the VSI injected voltage, hence the power angle is adjusted and the output power of the DG unit is also regulated such a way to maintain the microgrid active power balance. However, after the primary control action by LCs, steady-state system frequency may deviate from its reference set point value, in this case, the MGCC acts as a supervisory secondary controller to readjust the system frequency to the acceptable limits, which is performed by optimal regulation of DGs active power set-points as shown in Fig. 1. Moreover, the MGCC can also change the DG set-points owing to the EMS operational planning purposes. The supervisory control action of the MGCC is represented in general form by Eq. (3) in per-unit system.

$$\Delta P_g = \Delta P_{ref} - \frac{\Delta f}{m_p + D} \tag{3}$$

where ΔP_g, ΔP_{ref} and Δf are DG power output, DG power set-point and system frequency deviations adjustment performed by the MGCC, respectively. *D* also explains the microgrid load–frequency dependency coefficient. In short, regarding to Fig. 1., the EMS continuously monitors the microgrid power scheduling and energy flow and hence autonomously readjusts the reference power settings in accordance to its operational policies by properly employing the MGCC and LCs in a coherent hierarchical energy management structure.

Finally, it can be said the microgrid hierarchical frequency management structure is approximately the duality of the hierarchical frequency control framework performed in the transmission power systems [4–8]. Indeed, the primary control level of the microgrids is dual of the primary control level of the transmission power systems which is automatically performed by means of the synchronous generator governors [49]. In a microgrid, the secondary and some of the control functions of the tertiary control levels usually obtained by means of performance of the MGCC. Indeed, MGCC is responsible to readjust the voltage and frequency errors as the duality of the secondary control in the transmission systems. Additionally, it can pursue the operational purposes of the microgrid, such cost and emission optimization or running a security-constrained unit-commitment program which are usually performed in the tertiary control level of the transmission systems. Actually, the MGCC in a microgrid is equivalent with the Independent System Operator (ISO) or Transmission System Operator (TSO), which manages both the secondary and tertiary control functions [47–49]. However, in the microgrid, the control actions of the MGCC should be in coordination with the Distribution System Operator (DSO). DSO coordinates the operation of multi microgrids in the electricity market environment and over the wider distribution power systems. The performance of the DSO can also be included as a part of tertiary control level. As it has been also mentioned in the introduction, the performances of the secondary and tertiary control levels of the microgrids, are very close and interdependent and most of them are achieved by means of the MGCC.

3. Formulation of the proposed stochastic frequency control optimization

As mentioned above, the EMS is in charge of procurement sufficient reserve resources in the microgird to fulfill the operational goals in a secure and economical point of view. This function becomes more critical in the islanded mode, where system various uncertainties have more significant impacts on system frequency and consequently daily energy and reserve scheduling. To cope with such uncertainties arise from e.g. renewable energy source intermittent nature, load inevitable variations and/or system component outages, in this paper, a two-stage stochastic model for EMS is proposed such that system frequency excursions minimized in an economic–environmental framework. In the first stage, scenario generation using the RWM and LMCS strategies will be followed. To promote computational effort of the proposed model, a scenario reduction technique is also presented. Modeling of the MILP frequency control strategy over the reduced scenarios is performed in the second stage. The optimization problem is solved for each reduced scenario. Followings are the descriptions of the proposed two-stage stochastic frequency control optimization procedure.

3.1. First stage: Scenario generation and reduction

In this subsection, a brief overview of the proposed RWM and LMCS is presented, further descriptions in this issue can be found in the literature, e.g. in [50–55]. Inaccuracies in the forecasting values of renewable output generation and load consumption can be modeled as a continuous probability distribution function of the system forecasting errors. This probability distribution function, according to Fig. 2. can be discretized to some desired intervals with different standard deviation error with respect to zero error mean and also various probability dedicated to each interval. Then, RWM is employed to model the stochastic level of all considered uncertainties, i.e. wind turbine and photovoltaic panel power output variations, load fluctuations and possible system contingencies [53]. In this regard, initially, the range between [0, 1] is filled by normalized forecast errors probabilities as illustrated in Fig. 3. Then, over the path between [0, 1] a random number is generated.

If the generated random number falls into one of the normalized probability intervals in the roulette wheel path (here, the seven intervals), the RWM select that forecast error as a scenario. Notably, the summation of the normalized probabilities corresponding to the forecasted levels should become equal to one. On the other hand, to consider the uncertainties related to DG units outages, in each considered scenario, a random number in the range of [0, 1] is generated and compared to the FOR of each DG. If the produced random number is smaller than the corresponding FOR, the unit is out of service, otherwise, it means the unit is available. The procedure will be applied to the all DG units. A scenario in each hour of the optimization time horizon is a mix of the generated scenario by RWM for load, WT and PV forecasted errors and the determined status of each DG unit.

In this paper, due to higher convergence speed and smaller sampling dependency in similar conditions, LMCS method is employed instead of ordinary MCS for random number generation procedure. A ranked-r N-point lattice rule in d-dimension is calculated using Eq. (4) as follows [52,53]:

$$\left\{\sum_{l=1}^{r}\left(\frac{k_l}{n_l}\sum_{i=1}^{N}V_i\right)\mathrm{mod}1, \quad k_l = 1,\ldots,N \quad l = 1,\ldots,r\right\} \tag{4}$$

where V_1, $V_2, \ldots, V_N$ are independent integer d-dimensional randomly generated vectors by ordinary MCS, k_l and n_l are set of random numbers generate in range of [0–1] and an indicator to determine variation of k_l in rank l, respectively. n_1, $n_2, \ldots, n_r$ are set points of the LMCS and plays as input data of the LMCS. Total number of random values in each scenario and total generated scenario numbers by means of the LMCS are indicated by d and N parameters, respectively. Noteworthy, the N generated scenarios using the LMCS have more uniform distribution than the corresponding N scenarios in the ordinary MCS and consequently due to the covering the wider uncertainty spectrum, the LMCS leads to a more realistic solution [52].

Despite that the more generated scenarios yield the better modeling of uncertainties, to mitigate system complexity and computational volume, scenario reduction techniques are employed to eliminate the low probable and similar scenarios of the randomly generated scenarios in such a way system totality and uncertainty modeling be maintained suitably [52,53].

Concisely, in a 24-h period, after generating N scenarios for the first hour, by applying a scenario reduction technique, the remained NS scenarios are the basis for the scenario generation procedure in the next hour. Therefore, final system normalized scenario probability in period h and scenario s can be calculated as follows in Eq. (5) for a given seven interval probability distribution function:

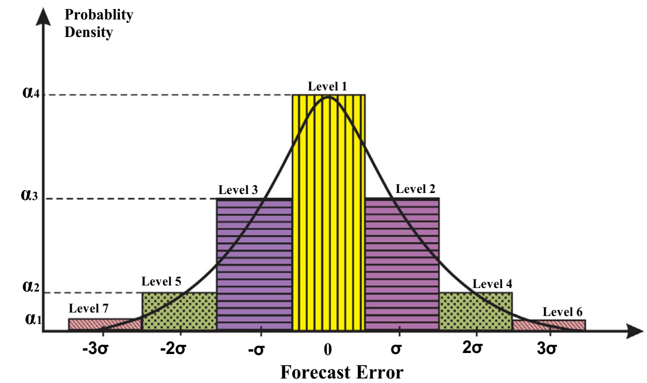

Fig. 2. Typical probability distribution function discretization of forecasting errors.

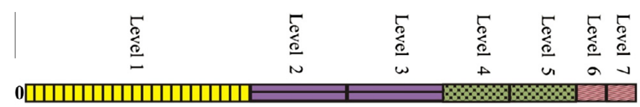

Fig. 3. The roulette wheel mechanism for the normalized forecasting errors.

$$\gamma^{DG}_{i,h,s} = \left(W^{DG}_{i,h,s}\cdot\left(1-\mathrm{FOR}^{DG}_i\right) + \left(1-W^{DG}_{i,h,s}\right)\cdot\mathrm{FOR}^{DG}_i\right)\times W^{DG}_{i,h-1,s} + \left(1-W^{DG}_{i,h-1,s}\right) \tag{6}$$

$W^{DG}_{i,h,s}$ is a randomly generated binary variable shows availability status of the ith DG unit at hour h and in scenario s, where, $W^{DG}_{i,h,s} = 1$ means that ith DG unit will be available in the hour h and scenario s and $W^{DG}_{i,h,s} = 0$ expresses that the DG unit i is out of service in the rest hours of the scheduling time horizon. FOR^{DG}_i is employed to explain Forced Outage Rate of ith DG unit.

Noteworthy, in Eq. (6) it is assumed that a DG unit after tripping will not be allowed to be in service in the last remained hours of the 24-h scheduling period. This means that if a DG unit trips at an hour, the probability of the removed units in the remained hours will be equal to 1, i.e. $\gamma_{i,h} = 1$ [53]. In should be noted that, Eq. (6) is the true only if the proposed sequential scenario generation procedure is implemented, i.e. the reduced generated scenarios in hour h are the basis for generating the scenario at next hour. In other words, the DG unit status at each hour should be determined considering to its status in the previous hour. Eq. (6) ensures this assumption. The adaptive scenario generation procedure is iterated over the considered 24-h period. To avoid the tautology, further explanation could be found in reference [52,53].

In this stage, system renewable energy source outputs, load level and available DG units are specified and the EMS is ready to schedule system energy and reserve resources in order to optimal control the system frequency excursions. In the following, the efficient linearized formulation of the proposed energy management system is precisely represented.

$$\pi_s = \frac{\prod_{h=1}^{Nh}\left(\left(\sum_{kl}^{7}W^{L}_{kl,h,s}\cdot\alpha_{kl,h}\right)\cdot\left(\sum_{kw=1}^{7}W^{WT}_{kw,h,s}\cdot\alpha_{kw,h}\right)\cdot\left(\sum_{kv=1}^{7}W^{PV}_{kv,h,s}\cdot\alpha_{kv,h}\right)\cdot\left(\prod_{i=1}^{Ng}\gamma^{DG}_{i,h,s}\right)\right)}{\sum_{s=1}^{Ns}\prod_{h=1}^{Nh}\left(\left(\sum_{kl}^{7}W^{L}_{kl,h,s}\cdot\alpha_{kl,h}\right)\cdot\left(\sum_{kw=1}^{7}W^{WT}_{kw,h,s}\cdot\alpha_{kw,h}\right)\cdot\left(\sum_{kv=1}^{7}W^{PV}_{kv,h,s}\cdot\alpha_{kv,h}\right)\cdot\left(\prod_{i=1}^{Ng}\gamma^{DG}_{i,h,s}\right)\right)}, \quad \forall s = 1,\ldots,Ns \tag{5}$$

where $W^{L}_{kl,h,s}$, $W^{WT}_{kw,h,s}$, $W^{PV}_{kv,h,s}$ are binary variables indicate the status of selection of klth load interval, kwth wind turbine power interval, kvth photovoltaic panel power interval in the hour h and scenario s, respectively. $\alpha_{kl,h}$, $\alpha_{kw,h}$ and $\alpha_{kv,h}$ are the probability of kl, kw and kv interval in the PDF of the forecasting error of load, wind output power and photovoltaic output power, respectively. $\gamma^{DG}_{i,h,s}$ denotes the share of DG units outage probability in π_s which can be also determined in a similar way using the applied RWM and LMCS strategies in a 24-h period according to Eq. (6):

3.2. Second stage: Stochastic MILP frequency control optimization

In this subsection, the optimization approach based on the system frequency excursions objective function will be described. The paper is aimed to minimized system frequency excursions of an islanded microgrid subject to the economic and environmental constraints which are dictated by mean of the EMS decision making strategies. Proposed optimization strategy is organized as following in Eq. (7):

$$\begin{aligned} &\min\ |\Delta f| \\ &s.t.\quad \textit{Total Operational Cost} \leqslant \textit{Cost}_{\max} \\ &\qquad \textit{Total System Emission} \leqslant \textit{Emission}_{\max} \end{aligned} \tag{7}$$

$Cost_{\max}$ and $Emission_{\max}$ criteria are maximum allowable cost and emission of operation imposed by the EMS decision makings in such a way that the microgrid operational goals will be insured, i.e. frequency excursion minimization is done subject to the economic and environmental constraints determined by higher level of the energy management system.

– *Objective function*

Expected absolute value of the System Frequency (ESF) as described in Eq. (8) is considered as the EMS main objective function to be minimized using an MILP based optimization over the 24-h scheduling horizon:

$$\mathrm{ESF} = \sum_{s=1}^{Ns} \pi_s \cdot \left(\sum_{h=1}^{Nh} \sum_{m} |\Delta f(s,m,h)| \right) \tag{8}$$

In order to formulate an MILP based optimization, preliminary, absolute function in $|\Delta f|$ must be linearized. In [47,48], it is assumed that the system frequency excursions are only occurred in the resultant of the synchronous generation unit outages as such the frequency excursions are always take negative values and nonlinear absolute function is spontaneously behaves linearly. However, if considerable renewable energy intermittencies and load variations are also considered, according to the droop control of DERs, Δf will take both negative and positive values. Thus, linear expression of $|\Delta f(s, m, h)|$ in Eq. (8), can be illustrated by the following substitutions as expressed by equation sets in Eq. (9) [56,57]:

$$|\Delta f(s,m,h)| = \Delta f^{+}(s,m,h) + \Delta f^{-}(s,m,h) \tag{9}$$

$$\Delta f(s,m,h) = \Delta f^{+}(s,m,h) - \Delta f^{-}(s,m,h)$$

$$\Delta f^{+}(s,m,h) \geqslant 0, \quad \Delta f^{-}(s,m,h) \geqslant 0$$

Therefore, using the applied linearization approach, both positive and negative frequency deviations can be aggregated in a linear form. Besides, there are several technical, economic and environmental constraints that must be taken into account by the energy management system which are restricting the microgrid proposed frequency control approach. These constraints must be also formulated in an MILP form.

3.2.1. Frequency droop control of inverter-interfaced DG units

According to Fig. 1, the steady-state frequency droop control behavior of a microgrid including inverter-interfaced DG units can be explained. In the primary control level corresponding to the distributed LCs action, the dispatchable DG units and the frequency elastic loads are automatically compensate frequency excursions as caused by the renewable energy source output power variations, system load fluctuations and the contingency events such as units/lines outages as represented in Eqs. (10) and (11). In this paper, it is assumed that nondispatchable renewable energy sources (wind turbines and photovoltaic panels) will not participate in the frequency control procedure of the microgrid and generate their stochastic active power output during each scenario, consequently, other DG units and controllable loads are responsible for the system frequency excursion compensation. On the other hand, the MGCC by optimally adjusting DG unit active power set points, corrects the steady-state system frequency deviations in an acceptable way such that not only the system frequency-based security guarantied but also the economical and environmental purposes of the system operation are suitably obtained.

$$\begin{aligned} \sum_{i=1}^{Ng} W^{DG}_{i,h,s} \cdot \Delta P_g(s,i,m,h) &= \Delta load(s,m,h) - \sum_{w=1}^{Nw} \Delta P_w(s,w,m,h) \\ &\quad - \sum_{v=1}^{Nv} \Delta P_v(s,v,m,h) \\ &\quad - \sum_{i=1}^{Ng} \left(1 - W^{DG}_{i,h,s}\right) \cdot \Delta P_g(s,i,m,h) \\ &\quad + D(s,m,h) \cdot \Delta f(s,m,h) - LSH(s,m,h) \end{aligned} \tag{10}$$

$$\begin{aligned} \sum_{i=1}^{Ng} \Delta P_g(s,i,m,h) &= \sum_{i=1}^{Ng} \Delta P_{ref}(s,i,m,h) - \sum_{i=1}^{Ng} \left(\frac{1}{m_p(i)} \right) \\ &\quad \cdot \Delta f(s,m,h) \quad \forall m = pri, \sec \end{aligned} \tag{11}$$

where $\Delta P(s, m, h) = P^s(m, h) - P(h)$ for all subscripts shows the active power deviation in response to the system frequency excursions. It should also be noted that in the primary interval similar to the normal operational conditions, reference power set point and the dispatched power output of the committed available DG units are exactly equal, thus, it can be concluded that:

$$\begin{aligned} P_{ref}(i,h) = P_g(i,h) \cdot u(i,h) \quad &\text{and} \quad W^{DG}_{i,h,s} \cdot P^s_{ref}(i,pri,h) \\ &= W^{DG}_{i,h,s} \cdot P^s_g(i,pri,h) \cdot u^{pri}(s,i,h). \end{aligned}$$

As described in Eq. (10), it is assumed that microgrid loads are elastic with respect to the system frequency and this elasticity can be calculated as in Eq. (12) for each hour and each control level in the steady state conditions:

$$D(s,m,h) = \frac{Load^s(m,h)}{f_{ref}} \tag{12}$$

Moreover, in the primary interval, owing to the automatic droop controller response of the DG units, there is not enough time for the EMS to change the commitment state of the DG units, thus, in the primary control level, both the commitment state and reference power set points of the DGs are constant, i.e. $W^{DG}_{i,h,s} \cdot u(i,h) = W^{DG}_{i,h,s} \cdot u^{pri}(s,i,h)$. Hence, the LC and MGCC control functions, i.e. the corresponding primary and secondary frequency control levels, respectively, are easily obtained from Eqs. (10) and (11) as illustrated by Eqs. (13) and (14).

$$\begin{aligned} &W^{DG}_{i,h,s} \cdot u^m(s,i,h) \cdot \left(\frac{1}{m_p(i)} \right) \cdot \Delta f(s,m,h) \\ &\quad = -W^{DG}_{i,h,s} \cdot \Delta P_g(s,i,m,h), \quad m = pri \end{aligned} \tag{13}$$

$$\begin{aligned} P^s_g(i,m,h) &= W^{DG}_{i,h,s} \cdot u^m(s,i,h) \\ &\quad \cdot \left[P^s_{ref}(i,m,h) - \left(\frac{1}{m_p(i)} \right) \cdot \Delta f(s,m,h) \right], \quad m = \sec \end{aligned} \tag{14}$$

Regarding to Eqs. (10)–(14), the system primary and secondary frequency excursions can be calculated considering to the active power deviations in the islanded microgrid with many parallel droop-controlled inverter interfaced DG units as follows in Eqs. (15) and (16):

$$\Delta f(s,m,h)|_{m=pri} = -\frac{\sum_{i=1}^{Ng} W^{DG}_{i,h,s} \cdot \Delta P_g(s,i,m,h)}{D(s,m,h) + \sum_{i=1}^{Ng} \frac{1}{m_p(i)} \cdot W^{DG}_{i,h,s} \cdot u^m(s,i,h)}, \quad m = pri \tag{15}$$

$$\Delta f(s,m,h)|_{m=\sec} = \frac{\sum_{i=1}^{Ng} W_{i,h,s}^{DG} \cdot [P_{ref}(s,i,m,h) - P_g(s,i,m,h)]}{D(s,m,h) + \sum_{i=1}^{Ng} \frac{1}{m_p(i)} \cdot W_{i,h,s}^{DG} \cdot u^m(s,i,h)}, \quad m = \sec \tag{16}$$

As it can be understood from Eqs. (11) and (12), in this paper, the load elasticity modeling is only considered in the primary control level in which the system frequency stability has extremely greater importance comparing to the secondary interval when the EMS has enough time to alleviate the frequency deviations by readjusting the reference power set-point of available DG units, hence the load elasticity has not been appeared in Eq. (16). Additionally, due to lower values of the microgrid secondary frequency excursions, the effect of load contribution is negligible with respect to the primary interval [47,48]. The amount of the primary load contribution $\Delta P^d(s,m,h)$ in the frequency control of each hour and in scenario s can be explained by Eq. (17).

$$\Delta P^d(s,m,h)|_{m=pri} = D(s,m,h)|_{m=pri} \cdot \Delta f(s,m,h)|_{m=pri} \tag{17}$$

To ensure that the system frequency deviates in an acceptable secure range, it is assumed that the microgrid primary and secondary frequency excursions must be smaller than the maximum allowable frequency excursion limits, such as inequalities illustrated by Eq. (18).

$$|\Delta f(s,m,h)| \leqslant \Delta f_m^{\max}, \quad \forall m = pri, \sec \tag{18}$$

Worth mentioning that due to the small capacity of DG units, in islanded mode of operation, all dispatchable units should participate in optimal energy and frequency based reserve management approach through the proposed hierarchical EMS approach. Furthermore, it is assumed that the nondispatchable units, i.e. Wind Turbines (WT) and Photovoltaic panels (PV) are dispatched in all hours by means of the EMS corresponding to their active power generation values in each reduced scenario.

3.2.2. Hourly power balance

The hourly power balance equations in the normal, primary and secondary intervals are described in Eqs. (19) and (20), respectively.

$$\sum_{i=1}^{Ng} P_g(i,h) + \sum_{w=1}^{Nw} P_w(w,h) + \sum_{v=1}^{Nv} P_v(v,h) = Load(h) \tag{19}$$

$$\sum_{i=1}^{Ng} P_g^s(i,m,h) + \sum_{w=1}^{Nw} P_w^s(w,m,h) + \sum_{v=1}^{Nv} P_v^s(v,m,h) = Load^s(m,h) + \Delta P^d(s,m,h) - LSH(s,m,h) \tag{20}$$

Moreover, to ensure that the optimal frequency dependent operation of the microgrid is within the determined security margins, the EMS have to unwillingly shed an amount of the microgrid total hourly load, if necessary, which can be described according to Eqs. (21) and (22).

$$LSH(s,m,h) = Load^s(m,h) - \sum_{i=1}^{Ng} P_g^s(i,m,h) - \sum_{w=1}^{Nw} P_w^s(w,m,h) - \sum_{v=1}^{Nv} P_v^s(v,m,h) - \Delta P^d(s,m,h) \tag{21}$$

$$0 \leqslant LSH(s,m,h) \leqslant Load^s(m,h) \tag{22}$$

3.2.3. Distributed generation units constraints

Total operation cost of each inverter interfaced DG unit is modeled as a first order continuous linear function of the active power output of the DG as described by Eqs. (23) and (24) for the normal, primary and secondary control level conditions, respectively:

$$Cost_g(i,h) = a_i \cdot u(i,h) + b_i \cdot P_g(i,h) + SUC_i \cdot y(i,h) + SDC_i \cdot z(i,h) \tag{23}$$

$$Cost_g^s(i,m,h) = a_i \cdot u^m(i,h) + b_i \cdot P_g^s(i,m,h) \tag{24}$$

Furthermore, total operation costs of the RESs are illustrated by Eqs. (25) and (26):

$$Cost_{res}(h) = \rho_w \cdot \sum_{w=1}^{Nw} P_w(w,h) + \rho_v \cdot \sum_{v=1}^{Nv} P_v(v,h) \tag{25}$$

$$Cost_{res}^s(m,h) = \rho_w \cdot \sum_{w=1}^{Nw} P_w^s(w,m,h) + \rho_v \cdot \sum_{v=1}^{Nv} P_v^s(v,m,h) \tag{26}$$

Cost of the scheduled up and/or down primary and secondary frequency control reserves for each DG unit in the scheduling time horizon which are applied by the LC and MGCC, respectively, is explained in Eq. (27):

$$Cost_R(i,m,q,h) = \rho_i(m,q) \cdot R_g(i,m,q,h) \tag{27}$$

Moreover, the active power output and scheduled primary and secondary reserves of available DG units must satisfy technical operational limits as follow in Eqs. (28)–(33):

$$P_g^{\min}(i) \cdot W_{i,h,s}^{DG} \cdot u(i,h) \leqslant P_g(i,h) \leqslant P_g^{\max} \cdot W_{i,h,s}^{DG} u(i,h) \tag{28}$$

$$P_g^{\min}(i) \cdot W_{i,h,s}^{DG} \cdot u^m(i,h) \leqslant P_g^s(i,m,h) \leqslant P_g^{\max}(i) \cdot W_{i,h,s}^{DG} u^m(i,h) \tag{29}$$

$$R_g(i,m,q,h)|_{\substack{m=pri\\q=up}} \geqslant W_{i,h,s}^{DG} \cdot \left(P_g^s(i,m,h)\Big|_{m=pri} - P_g(i,h) \right) \tag{30}$$

$$R_g(i,m,q,h)|_{\substack{m=pri\\q=dn}} \geqslant W_{i,h,s}^{DG} \cdot \left(P_g(i,h) - P_g^s(i,m,h)\Big|_{m=pri} \right) \tag{31}$$

$$R_g(i,m,q,h)|_{\substack{m=\sec\\q=up}} \geqslant W_{i,h,s}^{DG} \cdot \left(P_{ref}^s(i,m,h)\Big|_{m=\sec} - P_g(i,h) \right) \tag{32}$$

$$R_g(i,m,q,h)|_{\substack{m=\sec\\q=dn}} \geqslant W_{i,h,s}^{DG} \cdot \left(P_g(i,h) - P_{ref}^s(i,m,h)\Big|_{m=\sec} \right) \tag{33}$$

Eqs. (30)–(33) represent that DG units reserve amounts are determined according to the largest possible reserves among all selected scenarios in each hour for the microgrid power deviations in which the microgrid undergoes the most severe frequency excursions. Besides, the ramp up, ramp down, minimum up time and minimum down time limitations of the dispatchable DG units in the normal, primary and secondary intervals are linearized [57] and expressed through Eqs. (34)–(47):

$$P_g(i,h) - P_g(i,h-1) \leqslant RU_i \cdot (1 - y(i,h)) + RSU_i \cdot y(i,h) \tag{34}$$

$$P_g(i,h-1) - P_g(i,h) \leqslant RD_i \cdot (1 - z(i,h)) + RSD_i \cdot z(i,h) \tag{35}$$

$$y(i,h) - z(i,h) - u(i,h) + u(i,h-1) = 0 \tag{36}$$

$$y(i,h) + z(i,h) - 1 \leqslant 0 \tag{37}$$

$$P_g^s(i,m,h)\Big|_{m=pri} - P_g(i,h) \leqslant RU_i \cdot u(i,h) \tag{38}$$

$$P_g(i,h) - P_g^s(i,m,h)\Big|_{m=pri} \leqslant RD_i \cdot u(i,h) \tag{39}$$

$$P_g^s(i,m,h)\Big|_{m=\sec} - P_g^s(i,m,h)\Big|_{m=pri} \leqslant RU_i \cdot u^m(s,i,h)|_{m=pri} \tag{40}$$

$$P_g^s(i,m,h)\Big|_{m=pri} - P_g^s(i,m,h)\Big|_{m=\sec} \leqslant RD_i \cdot u^m(s,i,h)|_{m=\sec} \tag{41}$$

Minimum up/down time constraints:

$$\sum_{h=1}^{L_i}[1-u(i,h)]=0 \quad (42)$$

$$\sum_{\tau=h}^{h+TUP_i-1} u(i,h) \geqslant TUP_i y(i,h), \quad \forall h = L_i+1,\ldots,Nh-TUP_i+1 \quad (43)$$

$$\sum_{\tau=h}^{Nh}[u(i,h)-y(i,h)] \geqslant 0 \quad \forall h = Nh-TUP_i+2,\ldots,Nh \quad (44)$$

$$\sum_{h=1}^{K_i}u(i,h)=0 \quad (45)$$

$$\sum_{\tau=h}^{h+TDN_i-1}[1-u(i,h)] \geqslant TDN_i z(i,h), \quad \forall h = K_i+1,\ldots,Nh-TDN_i+1 \quad (46)$$

$$\sum_{\tau=h}^{Nh}[1-u(i,h)-z(i,h)] \geqslant 0 \quad \forall h = Nh-TDN_i+2,\ldots,Nh \quad (47)$$

where $L_i=\min\{Nh,(TUP_i-\delta_i^0)u(i,0)\}$; $K_i=\min\{Nh,(TDN_i-\sigma_i^0)(1-u(i,0))\}$.

Eqs. (42)–(44) are related to the minimum up time constraint which are enforce corresponding logics for hour 0, hours of size of TUP_i and the last TUP_i-1 h, respectively. Similarly, Eqs. (45)–(47) describe same logics for the minimum down time constraint [57]. Constants L_i and K_i represent initial periods in which DG unit i must be online and offline, respectively.

Total generated emission of the DG units assumed to be limited only to the CO_2 pollution as follows in Eqs. (48) and (49):

$$Emi_g(i,h)=E_i^{CO_2}\cdot P_g(i,h) \quad (48)$$

$$Emi_g^s(i,m,h)=E_i^{CO_2}\cdot P_g^s(i,m,h) \quad (49)$$

Finally, the day-ahead Total System Cost (TSC) and Total System Emission (TSE) of the microgrid regarding to the both normal condition and in the primary and secondary control levels are represented in Eqs. (50) and (51):

$$\mathrm{TSC}=\sum_{h=1}^{Nh}\left\{\sum_{i=1}^{Ng}Cost_g(i,h)+\sum_{i=1}^{Ng}\sum_{m}\sum_{q}Cost_R(i,m,q,h)+Cost_{res}(h)+\sum_{s=1}^{Ns}\pi_s\cdot\left[\sum_{i=1}^{Ng}\sum_{m}Cost_g^s(i,m,h)+\sum_{m}Cost_{res}^s(m,h)\right]\right\}+\mathrm{VOLL}\cdot\mathrm{ELNS} \quad (50)$$

$$\mathrm{TSE}=\sum_{h=1}^{Nh}\left\{\sum_{i=1}^{Ng}Emi_g(i,h)+\sum_{s=1}^{Ns}\pi_s\cdot\sum_{i=1}^{Ng}\sum_{m}Emi_g^s(i,m,h)\right\} \quad (51)$$

The description equation related to the system total Expected Load Not Served (ELNS) is calculated by Eq. (52):

$$\mathrm{ELNS}=\sum_{s=1}^{Ns}\sum_{m}\sum_{h=1}^{Nh}\pi_s\cdot LSH(s,m,h) \quad (52)$$

In the microgrid operational planning, the EMS can determine an appropriate framework according to the technical and economical policies in which the system be operated in a secure, cost-effective and emission-less manner. Hence, especially in the islanded mode, the EMS can give higher priority to control the system frequency excursions comparing to the economic and environmental objectives, therefore in this paper, it is assumed that the microgrid frequency will be controlled subject to the logical cost and emission limitations determined according to the EMS operational policies as explained in Eq. (7). The optimization constraints have been presented by Eqs. (9)–(52) and the objective function has been described by Eq. (8).

4. Simulation and numerical results

A modified low voltage microgrid consisted of five droop controlled inverter interfaced DG units, three wind turbines and two photovoltaic panels together with a group of radial distribution feeders is considered as the proposed islanded microgrid and illustrated in Fig. 4. The dispatchable DG units are included two 100 kW Fuel Cells (FC), two 150 kW Micro-Turbines (MT) and a 200 kW Gas Engine (GE) which are controlled by their interfaced VSI frequency droop controllers. Total installed capacity of WTs and PVs are 250 kW and 140 kW, respectively.

The technical and economical data related to the dispatchable DGs and also RESs including the fuel cost of energy and primary and secondary reserves, cost of start-up and shut-down, ramp up/down limits, minimum up/down times limits, frequency droop parameters (m_p) and CO_2 emission rates of the DGs have been listed in Tables 1 and 2 [42–44,59]. Worth to be mention, the frequency droop parameters of the dispatchable DGs have been set on 0.025 p.u. of their rated power in order to the power sharing procedure is performed proportionally to the DGs' capacity. In this study, the FOR of all DG units are assumed to be equal to 0.03. The cost of WTs and PVs active power generations, i.e. ρ_w and ρ_v, are 10.63 and 54.84 cents/kW h, respectively [44].

The forecasted values of the microgrid hourly load, WT and PV active power productions of the microgrid are depicted in Fig. 5.

The value of lost load (VOLL) has been selected as 1000 cent/kW h for all 24-h. Besides, in this study, 20 reduced scenarios consist of the microgrid aggregated load, RES power output and DG unit outage uncertainties are generated and have been applied to the proposed two-stage MILP stochastic optimization model. To

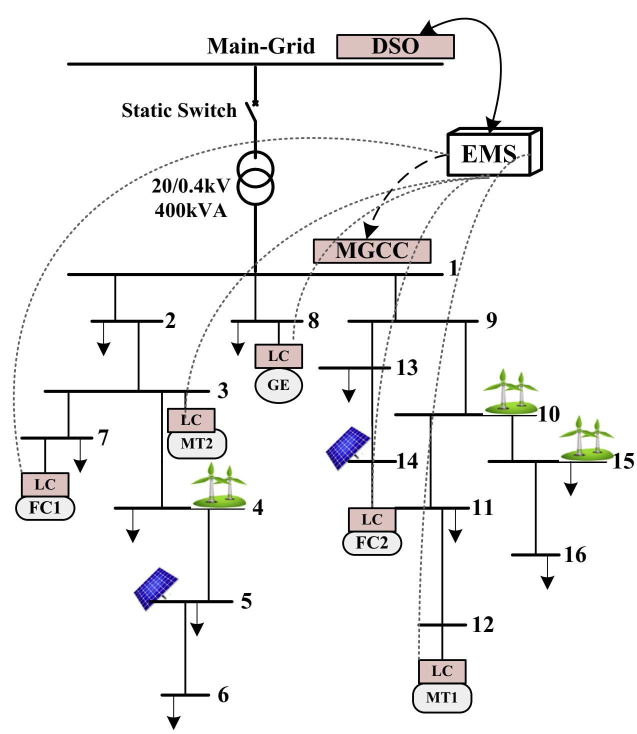

Fig. 4. The microgrid test system.

Table 1
The technical data of the microgrid dispatchable DG units.

DG unit	P_{gi}^{min} (kW)	P_{gi}^{max} (kW)	RU_i/RD_i (kW)	RSU_i/RSD_i (kW)	TUP_i/TDN_i (h)	m_p (mHz/kW)	$E_i^{CO_2}$ (kg/kW h)
MT1	25	150	100	150	2	1.000	0.550
MT2	30	150	100	150	2	1.000	0.550
FC1	30	100	100	100	2	1.500	0.377
FC2	20	100	100	100	2	1.500	0.377
GE	35	200	150	200	1	0.750	0.890

Table 2
The economic data of the microgrid dispatchable DG units.

DG unit	a_i (cents/h)	b_i (cents/kW h)	SUC_i (cents)	SDC_i (cents)	$\rho_i^{up/dn}(pri)$ (cents/kW h)	$\rho_i^{up/dn}(sec)$ (cents/kW h)
MT1	85.06	4.37	9	8	6.00	2.10
MT2	85.06	4.27	9	8	6.00	2.20
FC1	255.18	2.84	16	9	4.00	1.50
FC2	255.18	2.94	16	9	4.00	1.40
GE	212.00	3.12	12	8	3.80	1.70

construct the optimization model described briefly in Eq. (1), the EMS must have a deep insight into the microgrid operational aspects. Thus, in this paper, a pay-off table is first calculated by mean of the EMS regarding to the system main technical (ESF and ELNS), economic (TSC) and environmental (TSE) objective functions. The calculated pay-off table gives the upper and lower ranges of the system operational functions. Then, the EMS will make a decision based on the system operational policies to select the maximum allowable values of the microgrid economic–environmental restrictions from the constructed pay-off table through which the microgrid expected value of the frequency (ESF) be optimally managed and eventually the EMS overall policies appropriately satisfied.

In this paper, the numerical simulations of the proposed frequency dependent energy management system are presented in terms of two case studies. In both cases, economic–environmental constraints are imposed by means of the EMS regarding to the results in the corresponding payoff tables, however in Case I the secondary frequency excursion has been set in zero while this is allowed in Case II to the microgrid to experience ± 10 mHz frequency deviations in the secondary control level. The scheduled levels of energy and reserve values are illustrated in both cases and through some detailed analyzes, it is demonstrated that the EMS should pay more cost to sustain the system frequency excursions in a narrower limit as in Case I.

The simple calculated payoff tables in Case I (μ_{I}) and Case II (μ_{II}) in accordance to 4 important objective functions such that the microgrid overall operational aspects are satisfied are represented by μ_{I} and μ_{II}.

$$\mu_{\mathrm{I}} = \begin{bmatrix} obj \downarrow & \mathrm{TSC} & \mathrm{TSE} & \mathrm{ESF} & \mathrm{ELNS} \\ \mathrm{TSC} & 376852.891 & 16816.524 & 0.326 & 129.629 \\ \mathrm{TSE} & 7814455.701 & 8157.213 & 0.402 & 7589.961 \\ \mathrm{ESF} & 6339261.692 & 11428.164 & 0.047 & 6080.840 \\ \mathrm{ELNS} & 398952.441 & 16327.521 & 0.293 & 127.149 \end{bmatrix}$$

$$\mu_{\mathrm{II}} = \begin{bmatrix} obj \downarrow & \mathrm{TSC} & \mathrm{TSE} & \mathrm{ESF} & \mathrm{ELNS} \\ \mathrm{TSC} & 304512.936 & 17003.333 & 0.644 & 60.345 \\ \mathrm{TSE} & 8513123.839 & 7810.683 & 0.597 & 8289.474 \\ \mathrm{ESF} & 5803092.325 & 11419.589 & 0.047 & 5541.249 \\ \mathrm{ELNS} & 339549.532 & 15089.417 & 0.541 & 59.071 \end{bmatrix}$$

The fourfold considered objective functions are TSC, TSE, ESF and ELNS which are evaluated individually subject to the operational constraints in Section 4. In other words, each of objective functions are considered in sequence as the main fitness of the energy management system and the others are evaluated under that condition. For example, in μ_{I} when the ESF is the main fitness function, the optimization yields 0.047 as the minimum value of the expected frequency excursions while the corresponding cost, emission and ELNS of this frequency control are 6339261.692 cents, 11428.164 kg and 6080.840 kW h. This means that the EMS as the owner of the all DER units has to undertake an expensive opera-

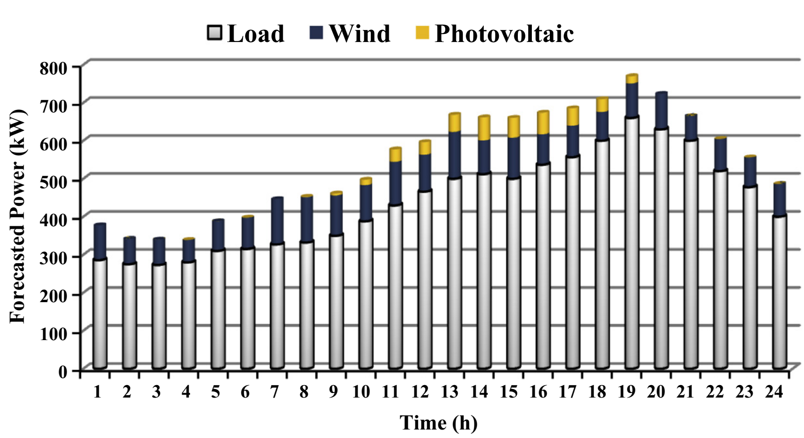

Fig. 5. Hourly forecasted values of load, wind turbine power output and photovoltaic power generation.

tional planning for the microgrid which is far from the ideal goals of the microgrid concept. The similar conditions are occurred in the Case II where the system frequency excursions can be changed over a wider secondary bound and again the cost of frequency excursion minimization will not justify the technical benefits of the microgrid frequency control. Thus, the EMS is in charge to provide an appropriate technical operational framework subject to its economic–environmental policies in which the microgrid frequency will be controlled optimistically in accordance to acceptable cost and emission restrictions. By this way, not only the microgrid frequency excursions are well managed considering to the allowable technical bounds, but also the system economic and environmental aspects are satisfied. In this paper, it is tried to select the cost and emission restrictions as narrow as possible such that the optimization procedure reaches to a feasible solution in a reasonable time. The selected values of economic and environmental restrictions by means of EMS cause the proposed MILP problem to be as a highly constrained optimization which should be solved with a powerful optimization tool. In this paper, the well-known powerful CPLEX solver is employed to solve the proposed problem in the GAMS environment [58]. The selected maximum values of system cost, emission, allowable ELNS and frequency excursions are listed in Table 1 for Case I and Case II. As it is obvious through μ_{I} and μ_{II} payoff tables, the microgrid will experience higher level of costs and emissions in Case I when the EMS enforces the secondary frequency excursions to be zero, this difference can imply that the cost of the frequency control action which is precisely presented by means of numerical results. As a result, the maximum allowable cost of frequency control is set in 400,000 cents in Case I in comparison to 335,000 cents in Case II. As it is observed in Table 3 the maximum levels of the microgrid cost, emission and ELNS limits are reasonably close to their optimal values in μ_{I} and μ_{II}.

The MILP optimization results of both Cases I and II in the terms of TSC, TSE, ESF and ELNS indices are list in Table 4. Moreover the details of cost the scheduled energy and reserve resources are presented in Table 4. Obviously, in Case II with allowable secondary frequency excursions within ±10 mHz, the cost of frequency control is lower comparing to the Case I where the EMS enforces the microgrid to set the secondary frequency deviations at zero. In other words, in Case II the EMS by adoption a conservative policy in the light of having greater secondary frequency excursions, not only manages the microgrid security in an appropriate manner, but also saves in operational costs within 64295.54 cent Day^{-1}.

In the following, the scheduled energy values of the microgrid dispatchable DG units in the Cases I and II are depicted in Fig. 6. All five DG units together with the RES units are dispatched properly to minimize the ESF in accordance to the EMS policies.

Table 3
The policies imposed by means of the EMS in Case I and Case II.

	TSC_{max} (cent)	TSE_{max} (kg)	$ELNS_{max}$ (kW h)	Δf_1^{max} (mHz)	Δf_2^{max} (mHz)
Case I	400,000	14,750	130	±35	0
Case II	335,000	15,000	70	±35	±10

The primary and secondary up/down frequency control reserves are represented in Figs. 7 and 8, respectively. According to the direction of the microgrid frequency excursions both up and down reserves have been scheduled to compensate the total power deviations in corresponding direction. In other words, whenever the microgrid undertakes positive frequency excursions the scheduled down reserves should be deployed to alleviate the frequency excursions while the scheduled up reserves are released for the sake of negative frequency excursion mitigation. The amounts of the scheduled primary reserves are proportionally to the microgrid frequency excursions and the droop coefficients of each DG unit. The hourly precise value of the scheduled up/down primary reserve for each DG unit is in proportion with largest negative/positive frequency excursion occurred in the reduced scenarios during each hour. The reference power set-point specified by the MGCC and the imposed operational policy by the EMS will determine the secondary control reserve amounts. Moreover, the EMS is in charge to dispatch the secondary control reserves between the DG units such a way both economical and security purposes will be achieved, although in this paper, the EMS focus is on the frequency control objectives.

In order to provide a thorough analysis of the proposed energy management system, the optimization results have been broken down in Table 5. The generation levels of the dispatchable DG units and RESs are represented in all 20 reduced scenarios for Case I and Case II. Besides, the absolute value of the microgrid expected frequency excursions and the amount of the expected load shed regarding to the primary and secondary control levels in each scenario is separately demonstrated. Noticeably, despite the strict secondary frequency limitation in the Case I, the amount of the expected load shed in the Case II and the microgrid overall operation costs are lower in all scenarios with respect to the Case I and the reason can be resulted from the DERs higher degrees of freedom to control the microgrid frequency due to the greater security margins dictated by mean of the EMS and thus this is a verification of that how much the EMS decision makings are productive in the microgrid operational planning. For example, in scenario S4, in which the microgrid experiences the outage of the FC2 for a 24-h time horizon, the amount of the primary and secondary load sheddings are lower in the Case II comparing to the Case I, because the performance of the available DG units in the secondary control level is developed by both the reference power set-point adjustment and releasing the stored energy in dc-link storage through the droop controller in accordance to the allowable secondary frequency excursion limit. Hence, the microgrid undertakes an acceptable frequency excursion in the secondary interval within 0.645 mHz per day, however, the this policy causes to higher microgrid exploitation from the DER capacities within 65.858 kW in the secondary control level and lower the involuntary load shedding within 2.575 kW, hence economizing the microgrid operation planning.

For a more detailed investigation, the microgrid energy management system performance in the scenario S2 with the highest probability and during three peak hours 18–20 is precisely assessed in the following. The amounts of the microgrid frequency excursions, load contribution, load shedding and variations in

Table 4
Day-ahead system optimization results.

Case	Energy cost		Reserve scheduling cost		Expected scenario generation cost				TSC (cent)	TSE (kg)	ESF (mHz)	ELNS (kW h)
					Primary		Secondary					
	DG	RES	Primary	Secondary	DG	RES	DG	RES				
I	50543.18	46399.93	13851.75	4937.37	50840.84	49872.74	53334.34	49872.74	398393.55	14701.78	0.241	128.60
II	50751.88	46399.93	14670.59	4732.81	52859.61	49872.74	52835.92	49872.74	334098.01	14971.61	0.263	61.96

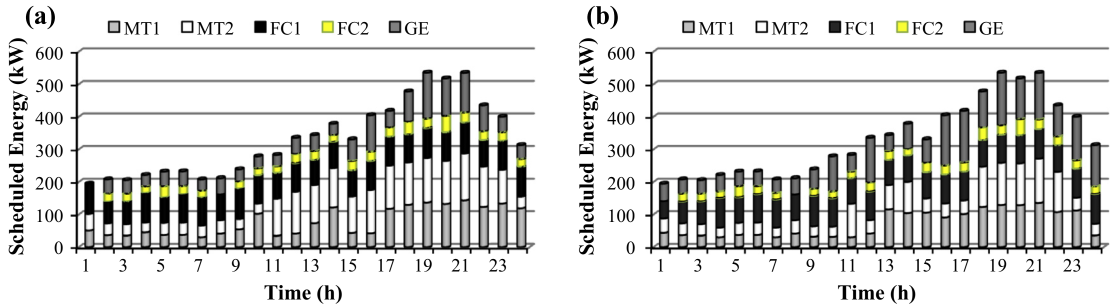

Fig. 6. The scheduled energy values of the microgrid dispatchable DG units: Case I (a) and Case II (b).

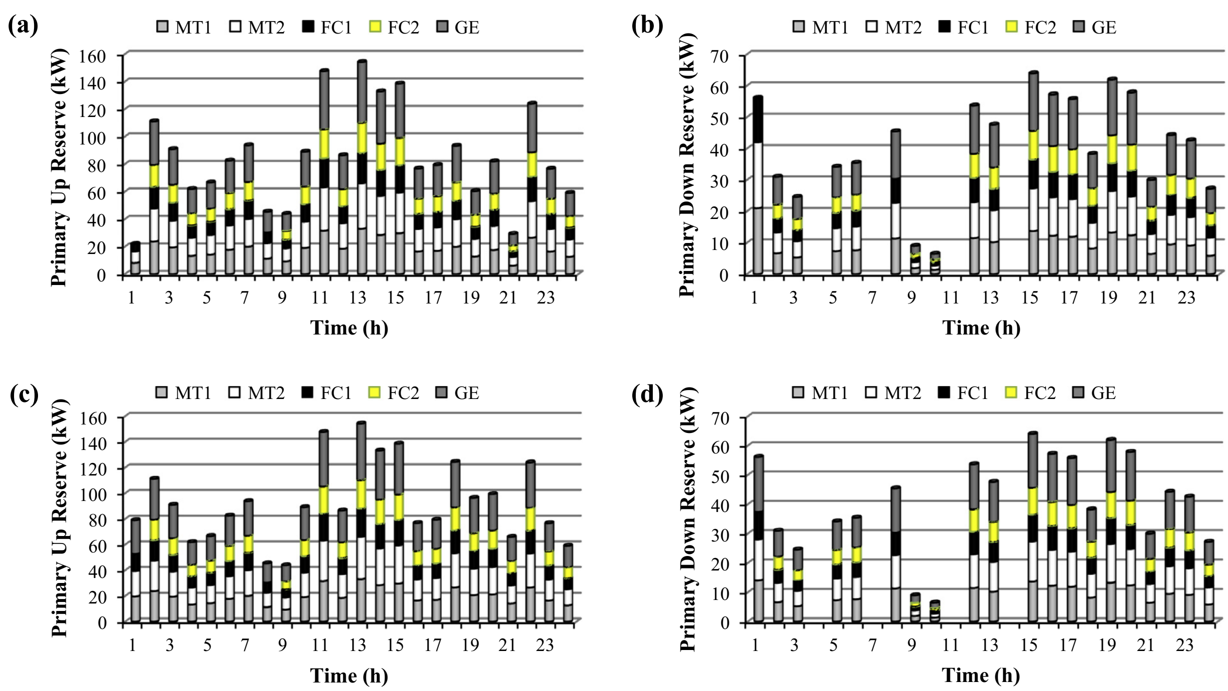

Fig. 7. The scheduled up and down primary frequency control reserves of the microgrid dispatchable DG units: Case I (a and b) and Case II (c and d).

renewable power generation and demand in scenario S2 during hour 18–20 are given in Table 6. According to Table 6, in hour 18, the microgrid total power variation is the summation of the stochastic ΔP_w, ΔP_v and $\Delta Load$ values (Eq. (10)) which yields to $120 - (18.18 + 9.9)$ (kW) in both cases. Hence, the committed available DG units should compensate the 91.92 kW, i.e., i.e. $\sum_{i=1}^{Ng} \Delta P_g(2, i, pri, 18) = 91.92$ kW. Regarding to the committed DG units at hour 18, thus, the primary frequency excursion is calculated using Eq. (15) which is extracted as follows:

$$\Delta f(2, pri, 18) = -\frac{91.92}{12 + (1/0.001 + 1/0.001 + 1/0.0015 + 1/0.0015 + 1/0.00075)} = -0.019646623 \text{ Hz}$$

This power deviations cause the microgrid primary frequency reaches to 59.980 Hz. The primary frequency excursion in hour 19 is positive because the total microgrid power variation is negative, i.e. $-33 - (21.84 + 7.14) = -61.98$ kW, thus in both cases the Δf_1 will be 13.251 mHz considering to the load sensitivity coefficient within 10.45 kW/Hz. Noticeably, when the system frequency excursion is positive, it means that the available DG units must decrease their power generation to compensate the occurred frequency excursion, hence, the DG units should provide down reserves as listed in Tables 7 and 8 for both Cases I and II. The loads contribution in the light of their frequency dependent characteristics is in such a way improving the primary response of the DG units, thus elastic loads automatically will increase their electrical consumption in the cases with positive frequency excursions to decrease the amount of deployed down reserves and consequently reduce the system operational costs. For example, in the Case I in hour 19, the primary frequency excursion without load dependency will be 13.281 mHz while it reduces to 13.251 mHz when the loads have been participated in the frequency control, although

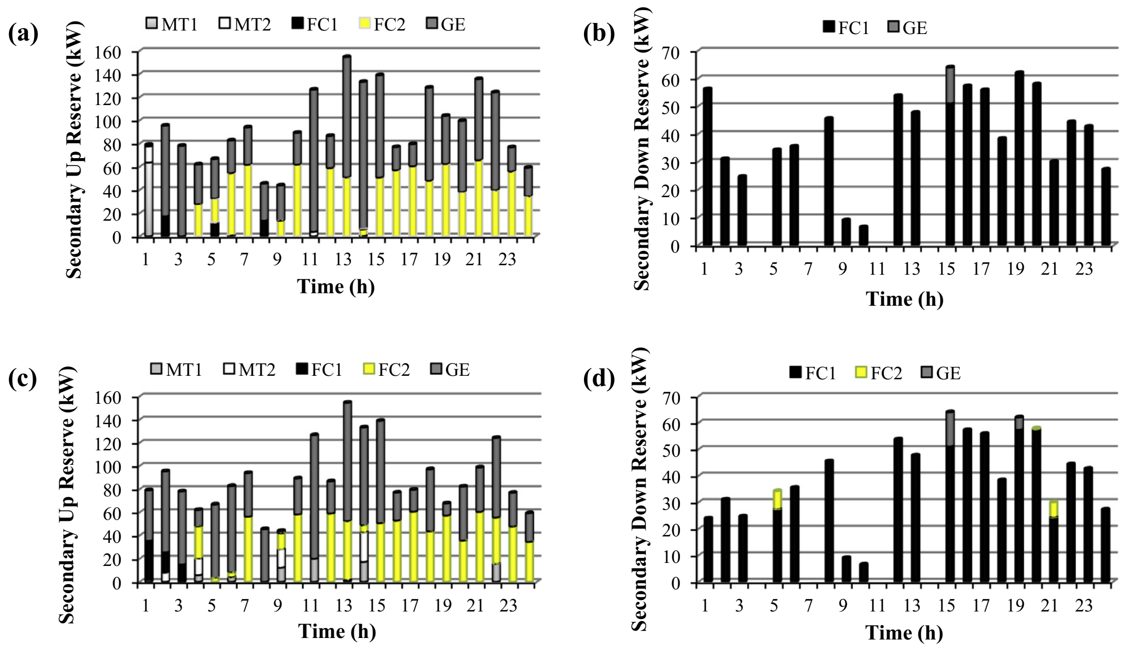

Fig. 8. The scheduled up and down secondary frequency control reserves of the microgrid dispatchable DG units: Case I (a and b) and Case II (c and d).

its active power seems to be negligible, however, it saves about 0.672 (cents) = 6 × (13.281 − 13.251) + 6 × (13.281 − 13.251) + 4 × (8.854 − 8.834) + 4 × (8.854 − 8.834) + 3.8 × (17.708 − 17.668) in the microgrid hourly primary reserve cost at hour 19.

In hour 20 and in Case I, total power variation equals to −126 + (22.38 + 3.99) = 99.63 kW, thus the microgrid frequency deviation according to Eq. (15) must be equal to −21.291 mHz as has been calculated in the Case II. Although the absolute value of the primary frequency excursion in the Case I is lower than the maximum allowable limit of the primary frequency excursion (35 mHz), however, as it is observed in Table 6 the microgrid has been undertook about 17.39 kW load shedding in the Case I. This occurred due to the physical limitations of the DG units. As illustrated in Table 6 at hour 20 in the Case I, the amount of scheduled energy of MT1 and MT2 are 132.424 kW and when they automatically response to the measured primary frequency excursion, according to Eq. (13), they must generate 132.424 + 0.0213021/0.001 = 153.726 kW which is greater than their maximum active power output limit, i.e. 150 kW. Similarly, FC1 also exceeds its upper physical limit, if it would participate in the primary frequency control action, i.e. 88.283 + 0.0213021/0.0015 = 102.487 which is greater than 100 kW. On the other hand, the free capacities of the two remained DG units, i.e. FC2 and GE have been dedicated to the their maximum primary and secondary control reserves, which enforces the EMS to involuntary shed about 17.39 kW of the microgrid hourly load to satisfy the system supply/demand balance constraint. In other words, because the primary frequency in the Case I has not been reached to the nadir point of the microgrid frequency, i.e. −35 mHz, it is first preferable to compensate frequency excursions by mean of available DG units, however, owing to the physical restrictions of available DG units, the EMS have to shed an amount of microgrid hourly load to maintain the system within the security margins. Thus, the new steady-state primary frequency excursion will be set in −17.575 mHz which can be calculated by Eqs. (21) and (15) and using the results given in Tables 7 and 8 and owing to the amounts of load consumption, wind turbines and photovoltaic panels power generations which are 756, 115.63 and 22.61 kW, respectively, as follows:

$$\begin{aligned} LSH(2,pri,20) &= 756 - [(150 + 150 + 100 + 61.606 + 138.541) \\ &\quad + 115.63 + 22.61 + 0.221] \\ &= -17.39\ \text{kW} \end{aligned}$$

$$\Delta f(2,pri,20) = -\frac{99.63 - 17.39}{12.6 + (1/0.001 + 1/0.001 + 1/0.0015 + 1/0.0015 + 1/0.00075)} = -0.017575404\ \text{Hz}$$

In Case II, owing to lower dispatched energy values of the committed DG units as illustrated in Table 7 in hour 20, there is no need to the load shedding and the available DG units are capable of alleviating the occurred primary frequency excursion within −21.291 mHz. Worth mentioning, by comparison between Tables 6 and 7 it can be understood due to allowable secondary frequency excursion, the amounts of provided energy of the DG units are lower in Case II with respect to the Case I, and therefore, the EMS has this opportunity to procure larger capacities for the primary and secondary reserves, thus not only the amounts of load shedding are reduced, but also there will be considerable saving in the system operation planning. Evidently, the reference power set-point specified by means of MGCC in the secondary control level in Case II is lower than in Case I, which can be observed in Tables 9 and 10.

Table 5
Day-ahead generation outputs, expected frequency excursion and expected load shed values in 20 reduced scenarios for Cases I and II.

Scenario number	Case	Total generation (kW)				Expected frequency excursion (mHz)		Expected load shed (kW)	
		Primary		Secondary					
		DG	RES	DG	RES	Primary	Secondary	Primary	Secondary
S1	I	9290.086	3189.360	9441.840	3189.360	9.383	0.000	4.749	0.000
	II	9394.298	3189.360	9441.679	3189.360	10.021	0.398	1.426	0.000
S2	I	9012.183	2958.540	9151.16	2958.540	63.109	0.000	28.472	0.000
	II	9079.515	2958.540	9151.019	2958.540	65.637	2.408	14.437	0.000
S3	I	8409.071	2553.840	8466.86	2553.840	18.069	0.000	3.817	0.000
	II	8465.982	2553.840	8466.860	2553.840	18.838	0.000	0.000	0.000
S4	I	8216.103	2272.170	8209.336	2272.170	8.455	0.000	3.260	3.587
	II	8216.399	2272.170	8275.194	2272.170	8.421	0.645	3.248	1.012
S5	I	8548.366	2673.590	8675.900	2673.590	3.936	0.000	2.389	0.117
	II	8610.635	2673.590	8682.242	2673.590	4.160	0.230	1.256	0.000
S6	I	8561.678	2828.855	8742.235	2828.855	4.854	0.000	3.945	0.000
	II	8666.057	2828.855	8741.970	2828.855	5.286	0.463	1.643	0.000
S7	I	8318.211	2851.928	8439.012	2851.928	7.456	0.000	4.441	0.000
	II	8386.329	2851.928	8438.891	2851.928	7.894	0.369	1.913	0.000
S8	I	8329.889	2645.968	8471.472	2645.968	17.234	0.000	12.517	0.830
	II	8397.565	2645.968	8481.302	2645.968	17.857	2.050	6.883	0.000
S9	I	9288.109	3189.360	9421.840	3189.360	3.512	0.000	1.572	0.000
	II	9374.358	3189.360	9421.726	3189.360	3.706	0.105	0.534	0.000
S10	I	8984.335	2986.440	9123.261	2986.440	7.281	0.000	3.285	0.000
	II	9051.667	2986.440	9123.119	2986.440	7.573	0.278	1.665	0.000
S11	I	8298.738	2664.380	8356.320	2664.380	13.726	0.000	2.905	0.000
	II	8355.650	2664.380	8356.320	2664.380	14.311	0.000	0.000	0.000
S12	I	8256.136	2351.830	8256.670	2351.830	5.680	0.000	0.000	0.000
	II	8256.141	2351.830	8256.670	2351.830	5.652	0.000	0.000	0.000
S13	I	8633.071	2661.550	8760.761	2661.550	7.991	0.000	5.044	0.247
	II	8695.338	2661.550	8767.102	2661.550	8.462	0.485	2.671	0.000
S14	I	8565.689	2824.835	8746.255	2824.835	5.826	0.000	4.662	0.000
	II	8670.068	2824.835	8745.990	2824.835	6.336	0.548	1.941	0.000
S15	I	8313.493	2815.428	8455.512	2815.428	18.263	0.000	13.457	0.890
	II	8381.611	2815.428	8465.309	2815.428	19.319	1.481	7.380	0.000
S16	I	8233.833	2665.708	8375.232	2665.708	9.054	0.000	6.635	0.441
	II	8301.517	2665.708	8385.043	2665.708	9.494	0.867	3.648	0.000
S17	I	8392.470	2643.840	8516.270	2643.840	2.333	0.000	1.721	0.000
	II	8451.471	2643.840	8516.177	2643.840	2.478	0.107	0.893	0.000
S18	I	8445.528	2849.395	8555.695	2849.395	16.640	0.000	8.412	0.000
	II	8490.864	2849.395	8555.602	2849.395	16.997	0.591	4.913	0.000
S19	I	8367.727	2891.548	8488.592	2891.548	5.017	0.000	2.880	0.000
	II	8435.845	2891.548	8488.471	2891.548	5.302	0.239	1.241	0.000
S20	I	8247.197	2638.548	8353.892	2638.548	13.155	0.000	7.669	0.660
	II	8283.862	2638.548	8363.803	2638.548	13.212	1.192	5.241	0.000

Table 6
Frequency excursion (mHz), system steady-state frequency (Hz), primary load contribution, load shedding, renewable power generation deviation and demand variation (kW) amounts in scenario 2 during hours 18–20.

Hour	Case	Δf_1	f_1	Δf_2	f_2	ΔP_{d1}	LSH_1	LSH_2	ΔP_w	ΔP_v	$\Delta Load$
Hour 18	I	−19.646	59.980	0	60	−0.235	0	0	18.18	9.9	120
	II	−19.646	59.980	0	60	−0.235	0	0	18.18	9.9	120
Hour 19	I	13.251	60.013	0	60	0.138	0	0	21.84	7.14	−33
	II	13.251	60.013	0	60	0.138	0	0	21.84	7.14	−33
Hour 20	I	−17.575	59.982	0	60	−0.221	17.39	0	22.38	3.99	126
	II	−21.291	59.978	−3.716	59.996	−0.268	0	0	22.38	3.99	126

Table 7
Scheduled energy, primary and secondary reserves at hours 18–20 in case I.

DG	Hour 18					Hour 19					Hour 20				
	Energy	Scheduled reserves				Energy	Scheduled reserves				Energy	Scheduled reserves			
		Primary		Secondary			Primary		Secondary			Primary		Secondary	
		Up	Down	Up	Down		Up	Down	Up	Down		Up	Down	Up	Down
MT1	129.345	20.019	8.186	0	0	137.115	12.884	13.251	0	0	132.424	17.575	12.374	0	0
MT2	129.345	20.019	8.186	0	0	137.115	12.884	13.251	0	0	132.424	17.575	12.374	0	0
FC1	86.230	13.346	5.457	0	38.280	91.410	8.760	8.834	0	61.980	88.283	11.716	8.249	0	57.870
FC2	28.834	13.346	5.457	48.129	0	28.835	8.760	8.834	62.405	0	49.890	11.716	8.249	38.171	0
GE	161.925	26.693	10.992	80.150	0	141.205	17.179	17.668	41.614	0	115.107	23.433	16.622	61.458	0

Table 8
Scheduled energy, primary and secondary reserves at hours 18–20 in case II.

DG	Hour 18					Hour 19					Hour 20				
	Energy	Scheduled reserves				Energy	Scheduled reserves				Energy	Scheduled reserves			
		Primary		Secondary			Primary		Secondary			Primary		Secondary	
		Up	Down	Up	Down		Up	Down	Up	Down		Up	Down	Up	Down
MT1	123.334	26.665	8.186	0	0	129.345	20.655	13.251	0	0	128.708	21.291	12.374	0	0
MT2	123.334	26.665	8.186	0	0	129.345	20.655	13.251	0	0	128.708	21.291	12.374	0	0
FC1	82.223	17.776	5.457	0	38.280	86.230	13.770	8.834	0	57.395	85.805	14.194	8.249	0	57.555
FC2	38.280	17.776	5.457	43.618	0	28.834	13.770	8.834	57.122	0	49.890	14.194	8.249	35.647	0.314
GE	110.877	35.553	10.992	53.569	0	161.925	27.540	17.668	10.534	4.584	125.018	28.389	16.622	46.592	0

Additionally, in Table 10 in hour 20, the secondary frequency excursion has been reached to the value of $\Delta f_1 = -3.716$ mHz, which can be calculated according to Eq. (16) and using the results listed in Table 8 as expressed in the following:

$$\Delta f(2, pri, 20) = -\frac{99.63 - 17.39}{12.6 + (1/0.001 + 1/0.001 + 1/0.0015 + 1/0.0015 + 1/0.00075)} = -0.017575404\ \text{Hz}$$

The steady-state frequency in analyzed peak hours in all 20 scenarios are shown in Fig. 9. As depicted in Fig. 9 the microgrid primary and secondary steady-state frequency in both Cases I and II are within the acceptable pre-specified secure ranges. As it can be seen, the frequency deviations in primary and secondary interval in Case II are larger comparing to the Case I. Because the secondary frequency deviations in Case I are set at zero, obviously, the steady-state secondary frequency in this case will set in 60 Hz, hence the related plot has not been illustrated.

Additionally, for a verification of the frequency control procedure in a more server power variation, the performance of the proposed energy management system in scenario S4 has been evaluated. In this scenario, the microgrid is not only exposed to renewable generation and load variations, but also a contingency has been occurred at hour 1 and the unit FC2 became unavailable for the remained hours, hence, other DG units have to appropriately mitigate the frequency deviations. For example, in hour 11, the load consumption increased about 86 kW, the wind generation decreased within 27.54 kW and photovoltaic output power increased about 6.9 kW. By outage of unit FC2 which was generating 20 kW, the amount of total power deviations becomes −126.64 kW, which causes the microgrid frequency gets the 59.968 Hz in steady-state. Thus, other available DG units must provide adequate up reserves to optimally control the −31.592 mHz frequency excursion. Evidently, FC2 has not been participated in the primary and secondary control levels and the EMS has dispatched other DG units in both cases according to the economic–environmental policies of each case. The generation levels in this scenario are listed in Table 11.

Table 9
DG unit primary and secondary generation levels and MGCC reference power set-point (kW) in scenario S2 during peak hours (18–20) in Case I.

DG	Hour 18			Hour 19			Hour 20		
	Generation level		MGCC reference power set-point	Generation level		MGCC reference power set-point	Generation level		MGCC reference power set-point
	Primary	Secondary		Primary	Secondary		Primary	Secondary	
MT1	149.6267	129.980	129.980	123.863	137.115	137.115	150	132.414	132.424
MT2	149.6267	129.980	129.980	123.863	137.115	137.115	150	132.414	132.424
FC1	99.751	50.293	50.293	82.575	29.430	29.430	100	88.276	88.283
FC2	51.377	86.409	86.409	20	28.835	28.835	61.606	88.008	88.061
GE	119.352	173.306	173.306	123.537	141.205	141.205	138.541	176.552	176.566

Table 10
DG unit primary and secondary generation levels and MGCC reference power set-point (kW) in scenario 2 during peak hours (18–20) in Case II.

DG	Hour 18			Hour 19			Hour 20		
	Generation level		MGCC reference power set-point	Generation level		MGCC reference power set-point	Generation level		MGCC reference power set-point
	Primary	Secondary		Primary	Secondary		Primary	Secondary	
MT1	142.981	123.334	123.334	116.093	129.345	129.345	150	132.424	128.708
MT2	142.981	123.334	123.334	116.093	129.345	129.345	150	132.424	128.708
FC1	95.320	82.223	82.223	77.395	28.834	28.834	100	88.283	85.805
FC2	51.377	81.898	81.898	20	28.834	28.834	64.084	88.014	85.537
GE	137.072	159.178	159.178	144.257	157.341	157.341	153.407	176.566	171.610

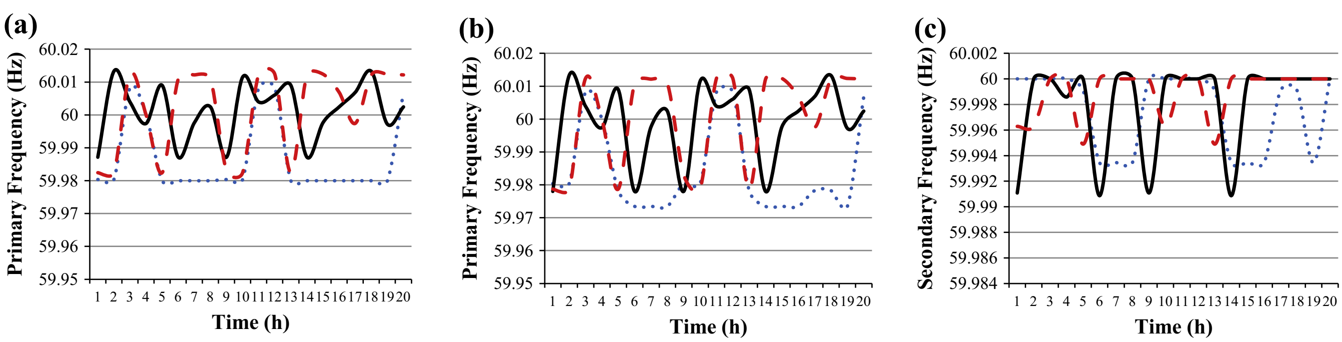

Fig. 9. Microgrid primary and secondary steady-state frequency during peak hours 18–20 in all 20 scenarios; hour 18 (dotted), hour 19 (solid), hour 20 (dashed): Case I (a), Case II (b and c).

Table 11
The optimization results in scenario S4 at hour 11 in Cases I and II.

DG	Energy	Energy	Scheduled Up-Reserve				Generation level				MGCC reference power set-point	
			Primary		Secondary		Primary		Secondary			
Case	I	II	I	II	I	II	I	II	I	II	I	II
MT1	34.738	30	31.592	31.592	0	20	66.330	61.592	34.738	50	34.738	50
MT2	114.373	103.145	31.592	31.592	4.034	0	145.965	134.737	118.407	103.145	118.407	103.145
FC1	78.938	78.938	21.061	21.061	0	0	100	100	78.938	78.938	78.938	78.938
FC2	20	20	21.061	21.061	0	0	0	0	0	0	0	0
GE	35	50.965	42.394	42.394	122.605	106.640	77.122	93.088	157.605	157.605	157.605	157.605

5. Conclusions

This paper addressed the precise modeling of the frequency dependent behavior of the droop controlled microgrids. A two-stage stochastic optimization framework has been employed to be minimized the expected value of system frequency excursions. In first stage, using the RWM and LMCS strategies, some randomly scenarios corresponding to the wind and photovoltaic intermittent power outputs, load demand fluctuations and distributed generation unit outages were generated and properly reduced. Then 20 remained scenarios applied to the second stage of optimization. In this stage, a mixed-integer linear programming approach was formulated effectively to solve the proposed energy management system. Besides the frequency-droop control paradigms of the inverter-interfaced DG units have been precisely derived and incorporated into the day-ahead reserve management framework. A novel objective function in the terms of expected system frequency (ESF) has been constructed and aimed to be minimized subject to the imposed economic–environmental policies pre-specified by means of the EMS. To thoroughly investigate the proposed frequency management system, two case-studies have been defined over a typical test system in a 24-h period. Numerical results corresponding to the provided energy and scheduled primary and secondary control reserves were demonstrated comprehensively. In first case study, the microgrid secondary frequency have been controlled at its rated value. In this regard, the MGCC adjusted the active power set points such that the desired restrictions were preserved. The results showed that in order to set the secondary frequency excursions at the exactly zero value, the EMS has to pay more costs with respect to the second case-study in which the microgrid was allowed to experience wider secondary frequency excursions. Moreover, the microgrid load–frequency dependency was modeled precisely and the loads natural response to simulated frequency excursions has been assessed in-depth. The EMS should undertake higher level of emission and costs when the load–frequency dependency is neglected. Numerical results were presented and analyzed in detail over all scenarios. The amounts of the primary and secondary control reserves provided by the LCs and MGCC performance were calculated. Worth mentioning that the frequency dependent modeling has direct impact on the amounts of the scheduled control reserves, provided energy and even the commitment state of the microgrid. Reference active power set-points were determined in an optimistic way by the MGCC to adjust the microgrid frequency excursions in the acceptable ranges. Obviously, in the second case-study where the frequency was not obliged to be managed at the exactly rated value, the costs related to the adjustment of the reference power setting and also the deployment of the primary and secondary control reserves were decreased significantly. Productivity of the proposed frequency aware energy management system in increasing the power system security margins verifies the great importance of the precise frequency modeling in the operational planning studies of the microgrids.

References

[1] Katiraei F, Iravani R, Hatziargyriou N, Dimeas A. Microgrids management. IEEE Power Energy Mag 2008;6(3):54–65.

[2] Lasseter RH, Paigi P. Microgrid: a conceptual solution. In: Proceeding of 35th annual IEEE power electronics specialists conference; 2004. p. 4285–90.

[3] Hatziargyriou N, Asano H, Iravani R, Marnary C. Microgrids. IEEE Power Energy Mag 2007;5(4):78–94.

[4] Jimeno J, Anduaga J, Oyarzabal J, de Muro AG. Architecture of a microgrid energy management system. Eur Trans Electr Eng 2011;21:1142–58.

[5] Vandoorn TL, Vasquez JC, Kooning JD, Guerrero JM, Vandevelde L. Microgrids: hierarchical control and on overview of the control and reserve management strategies. IEEE Ind Electron Mag 2013:42–55.

[6] Guerrero JM, Chandorkar M, Lee TL, Loh PC. Advanced control architecture for intelligent microgrids – Part I: Decentralized and hierarchical control. IEEE Trans Industr Electron 2013;60(4):1254–62.

[7] Simpson-Porco JW, Dorfler F, Bullo F. Synchronization and power sharing for droop-controlled inverters in islanded microgrids. Automatica 2013;49(9):2603–11.

[8] Olivares DE, Canizares CA, Kazerani M. A centralized optimal energy management system for microgrids. In: IEEE PES general meeting; 2011. p. 1–6.

[9] Guerrero JM, Vasquez JC, Matas J, de Vicuna LG, Castilla M. Hierarchical control of droop-controlled AC and DC microgrids – a general approach toward standardization. IEEE Trans Industr Electron 2011;58(1):387–405.

[10] Justo JJ, Mwasillu F, Lee J, Jung JW. AC-microgrids versus DC-microgrids with distributed energy resources: a review. Renew Sustain Energy Rev 2013;24:387–405.

[11] Palizban O, Kauhaniemi K, Guerrero JM. Microgrids in active network management – Part I: Hierarchical control, energy storage, virtual power plants, and market participation. Renew Sustain Energy Rev 2014. Early access.

[12] Rocabert J, Luna A, Blaabjerg F, Rudriguez P. Control of power converters in AC microgrids. IEEE Trans Power Electron 2012;27(11):4734–49.

[13] Lopez JAP, Moreira CL, Madureira AG. Defining control strategies for microgrids islanded operation. IEEE Trans Power Syst 2006;21(2):916–24.

[14] Bidram A, Davoudi A. Hierarchical structure of microgrids control system. IEEE Trans Smart Grid 2012;3(4):1963–76.

[15] Planas E, de Muro AG, Andreu J, Kortabarria I, de Alegria IM. General aspects, hierarchical controls and droop methods in microgrids: a review. Renew Sustain Energy Rev 2013;17:147–59.

[16] De D, Ramanarayanan V. Decentralized parallel operation of inverters sharing unbalanced and nonlinear loads. IEEE Trans Power Electron 2010;25(12):3015–25.

[17] Mohd A, Ortjohann E, Morton D, Omari O. Review of control techniques for inverter parallel operation. Electr Power Syst Res 2010;80(12):1477–87.

[18] Chandorkar MC, Divan DM, Adapa R. Control of parallel connected inverters in standalone AC supply systems. IEEE Trans Ind Appl 1993;29(1):136–43.

[19] Eid BL, Rahim NA, Selvaraj J, Al Khateb AH. Control methods and objectives for electronically coupled distributed energy resources in microgrids: a review. IEEE Syst J 2014:1–13. Early access.

[20] Hatziargyriou ND. Microgrids and energy management. Eur Trans Electr Power 2011:1139–42. Special issue.

[21] Moghaddam AA, Seifi A, Niknam T, Alizadeh Pahlavani MR. Multi-objective operation management of a renewable microgrid with back-up micro-turbine/fuel cell/battery hybrid power source. Energy 2011;36:6490–507.

[22] Chen C, Duan S, Cai T, Liu B, Hu G. Smart energy management strategy for optimal microgrid economic operation. IET Renew Power Gener 2011;5(3):258–67.

[23] Mohammad FA, Koivo HN. Online management genetic algorithms of microgrid for residential application. Energy Convers Manage 2012;64:562–8.

[24] Zhang L, Gari N, Hmurcik LV. Energy management in a microgrid with distributed energy resources. Energy Convers Manage 2014;78:297–305.

[25] Mohammadi S, Soleymani S, Mozafari B. Scenario-based stochastic operation management of microgrid including wind, photovoltaic, micro-turbine, fuel cell and energy storage devices. Int J Electr Power Energy Syst 2014;54:525–35.

[26] Niknam T, Azizipanah R, Narimani MR. An efficient scenario-based stochastic programming framework for multi-objective optimal microgrid operation. Appl Energy 2012;99:455–70.

[27] Motavasel M, Seifi AR. Expert energy management of a microgrid considering wind energy uncertainty. Energy Convers Manage 2014;83:58–72.

[28] Mohammadi S, Mozafari B, Niknam T. An adaptive modified firefly optimisation algorithm based on Hong's point estimate method to optimal operation management in a microgrid with consideration of uncertainties. Energy 2013;51:339–48.

[29] Mohammadi S, Mozafari B, Soleymani S. A stochastic programming approach for optimal microgrid economic operation under uncertainty using 2m+ 1 point estimate method. J Renew Sustain Energy 2013;5(3):033112.

[30] Mohammadi S, Mozafari B, Solymani S, Niknam T. Stochastic scenario-based model and investigating size of energy storages for PEM-fuel cell unit commitment of micro-grid considering profitable strategies. IET Gen Trans Distrib 2014;8(7):1228–43.

[31] Chen Y, Lu S, Chang Y, Lee T, Huc M. Economic analysis and optimal energy management models for microgrid systems: a case study in Taiwan. Appl Energy 2013;103:14554.

[32] Prodan I, Zio E. A model predictive control framework for reliable microgrid energy management. Int J Electr Power Energy Syst 2014;61:399–409.

[33] Marzband M, Sumper A, Ruiz-Alvarez A, Garcia JLD, Tomoiuga B. Experimental evaluation of a real time energy management system for stand-alone microgrids in day-ahead markets. Appl Energy 2013;106:365–76.

[34] Marzband M, Sumper A, Garcia JLD, Ferret RG. Experimental validation of a real time energy management system for microgrids in islanded mode using a local day-ahead electricity market and MINLP. Energy Convers Manage 2013;76:314–22.

[35] Zakariazadeh A, Jadid S, Siano P. Economic–environmental energy and reserve scheduling of smart distribution systems: a multi-objective mathematical programming approach. Energy Convers Manage 2014;78:151–64.

[36] Zakariazadeh A, Jadid S, Siano P. Multi-objective scheduling of electric vehicles in smart distribution systems. Energy Convers Manage 2014;79:43–53.

[37] Palma-Behnke R, Benavides C, Lanas F, Severino B, Reyes L, Llanos J, et al. A microgrid energy management system based on rolling horizon strategy. IEEE Trans Smart Grid 2013;4(2):996–1006.

[38] Barklund E, Pogaku N, Prodanovic M, Hernandez-Aramburo E, Green TC. Energy management in autonomous microgrid using stability constraint droop control of inverters. IEEE Trans Power Electron 2008;23(5):2346–52.

[39] Hernandez-Aramburo CA, Green TC, Mugniot N. Fuel consumption minimization of a microgrid. IEEE Trans Ind Appl 2005;41(3):673–81.

[40] Divshali PH, Hosseinian SH, Abedi M. A novel multi-stage fuel cost minimization in a VSC-based microgrid considering stability, frequency and voltage constraints. IEEE Trans Power Syst 2013;28(2):931–9.

[41] Katiraei F, Iravani MR. Power management strategies for a microgrid with multiple distributed generation units. IEEE Trans Power Syst 2006;21(4):1821–31.

[42] Jiang Q, Xue M, Geng G. Energy management of microgrid in grid-connected and islanded modes. IEEE Trans Power Syst 2013;28(3):3380–9.

[43] Conti S, Nicolosi R, Rizzo SA, Zeineldin HH. Optimal dispatching of distributed generators and storage systems for MV islanded microgrids. IEEE Trans Power Delivery 2012;27(3):1243–51.

[44] Tsikalakis AG, Hatziargyriou ND. Centralized control for optimizing microgrids operation. IEEE Trans Energy Convers 2008;23(1):241–8.

[45] Olivares DE, Canizares CA, Kazerani M. A centralized energy management system for isolated microgrids. IEEE Trans Smart Grid 2014;5(4):1864–75.

[46] Wood AJ, Wollenberg BF. Power generation, operation and control. New York: Willey; 1984.

[47] Galiana FD, Bouffard F, Arroyo JM, Restrepo JF. Scheduling and pricing of coupled energy and primary, secondary and tertiary reserves. Proc IEEE 2005;93(11):1970–83.

[48] Rabbanifar P, Jadid S. Stochastic multi-objective security-constrained market clearing considering static frequency of power system. Int J Electr Power Energy Syst 2014;54:465–80.
[49] Malik O, Havel P. Decision support tool for optimal dispatch of tertiary control reserves. Int J Electr Power Energy Syst 2012;42:341–9.
[50] Michalewicz Z. Genetic algorithm + data structure = evaluation program. New York (USA): Springer-Verlag; 1996.
[51] Billinton R, Allan RN. Reliability evaluation of power systems. New York (USA): Plenum; 1996.
[52] Esmaili M, Amjady N, Shayanfar HA. Stochastic congestion management in power markets using efficient scenario approaches. Energy Convers Manage 2010;51:2285–93.
[53] Aghaei J, Karami M, Muttaqi KM, Shayanfar HA, Ahmadi A. MIP-based stochastic security-constrained daily hydrothermal generation scheduling. IEEE Syst J 2014:1–14. Early access.
[54] Wu L, Shahidehpour M, Li T. Cost of reliability analysis based on stochastic unit commitment. IEEE Trans Power Syst 2008;23(3):1364–74.
[55] Conejo AJ, Milano F, García-Bertrand R. Congestion management ensuring voltage stability. IEEE Trans Power Syst 2006;21(1):357–64.
[56] Castillo E, Conejo AJ, Pedregal P, Garcia R, Alguacil N. Building and solving mathematical programming models in engineering and science. New York: Willey; 2011.
[57] Motto AL, Galiana FD, Conejo AJ, Arroyo JM. Network-constrained multi period auction for a pool-based electricity market. IEEE Trans Power Syst 2002;17(3):646–53.
[58] Generalized Algebraic Modeling Systems (GAMS) <http://www.GAMS.com>.
[59] Shi L, Luo Y, Tu GY. Bidding strategy of microgrid with consideration of uncertainty for participating in power market. Int J Electr Power Energy Syst 2014;59:1–13.